

RESEARCH ARTICLE

Gills versus kidney for ionoregulation in the obligate air-breathing *Arapaima gigas*, a fish with a kidney in its air-breathing organ

Chris M. Wood^{1,2,*}, Bernd Pelster^{3,4}, Susana Braz-Mota⁵ and Adalberto L. Val⁵

ABSTRACT

In *Arapaima gigas*, an obligate air-breather endemic to ion-poor Amazonian waters, a large complex kidney runs through the air-breathing organ (ABO). Previous indirect evidence suggested that the kidney, relative to the small gills, may be exceptionally important in ionoregulation and nitrogen (N) waste excretion, with support of kidney function by direct O₂ supply from the airspace. We tested these ideas by continuous urine collection and gill flux measurements in ~700 g fish. ATPase activities were many-fold greater in kidney than gills. In normoxia, gill Na⁺ influx and efflux were in balance, with net losses of Cl⁻ and K⁺. Urine flow rate (UFR, ~11 ml kg⁻¹ h⁻¹) and urinary ions (< 0.2 mmol l⁻¹) were exceptional, with [urine]:[plasma] ratios of 0.02–0.002 for K⁺, Na⁺, and Cl⁻, indicating strong reabsorption with negligible urinary ion losses. Urinary [ammonia] was very high (10 mmol l⁻¹, [urine]:[plasma] ~17) indicating strong secretion. The kidney accounted for 21–24% of N excretion, with ammonia dominating (95%) over urea-N through both routes. High urinary [ammonia] was coupled to high urinary [HCO₃⁻]. Aerial hypoxia (15.3 kPa) and aerial hyperoxia (>40.9 kPa) had no effects on UFR, but both inhibited branchial Na⁺ influx, revealing novel aspects of the osmorepiratory compromise. Aquatic hypoxia (4.1 kPa), but not aquatic hyperoxia (>40.9 kPa), inhibited gill Na⁺ influx, UFR and branchial and urinary ammonia excretion. We conclude that the kidney is more important than gills in ionoregulation, and is significant in N excretion. Although not definitive, our results do not indicate direct O₂ supply from the ABO for kidney function.

KEY WORDS: ABO, Gills, Hyperoxia, Ammonia, Hypoxia, Osmorepiratory compromise, Paiche, Pirarucu, Sodium fluxes, Urea-N, Urine

INTRODUCTION

Arapaima gigas ('pirarucu') is endemic to the Amazon watershed and is the largest freshwater fish ever found in the wild. It is now farmed extensively in aquaculture. It starts life as a water-breather (Graham, 1997), but within a few weeks after hatching, the pirarucu becomes an obligate air-breather that will quickly drown if denied access to air (Brauner et al., 2004; Brauner and Val, 1996). In older animals, there is a very large, well vascularized and greatly

invaginated air-breathing organ (ABO, often termed a 'lung') that runs the entire length of the abdominal cavity (Hochachka et al., 1978; Soares et al., 2006; Fernandes et al., 2012; Scadenga et al., 2020). The ABO becomes the dominant site of O₂ uptake (\dot{M}_{O_2}) accounting for 60–80% of the total, while the gills are retained as the major sites of CO₂ excretion (\dot{M}_{CO_2}), accounting for 60–90% of the total (Stevens and Holeyton, 1978; Brauner and Val, 1996; Gonzalez et al., 2010; Pelster et al., 2020a). It is generally believed that the gills also remain the major sites of ionoregulation, a critical function in light of the ion-poor nature of Amazonian waters (Val and Almeida-Val, 1995; Gonzalez et al., 2005), as well as the major site of nitrogenous waste excretion in these high protein-consuming carnivores. However, as discussed subsequently, the evidence is less clear on these points.

An unusual anatomical feature of the ABO that has fascinated morphologists for many years is the large kidney contained within it (for photographs and diagrams, see Hochachka et al., 1978; Fernandes et al., 2012; Scadenga et al., 2020). This kidney is similarly well vascularized, and engorged with blood in freshly dissected specimens. It runs in two strap-like bands along the dorsal surface of the ABO, and is enveloped by the respiratory parenchyma (Fernandes et al., 2012). Pelster and Wood (2018) noted 'it is hard to believe that there is not a mechanistic, functional relationship between the two organs, though this has never been investigated'. Perhaps O₂ can diffuse directly from the ABO airspace into blood vessels in the kidney, and/or perhaps there are direct connections between blood vessels in the ABO and kidney. Therefore our first hypothesis was that O₂ levels in the ABO would affect the active transport functions of ion reabsorption and nitrogenous waste (N-waste) secretion in the kidney.

The mass-specific gill surface area becomes progressively reduced and water-to-blood diffusion distance increases as development proceeds because the secondary lamellae are obliterated by infilling with the inter-lamellar cell mass (Hulbert et al., 1978b; Brauner et al., 2004; Ramos et al., 2013). This, together with the large size and complex structure of the kidney, an abundance of mitochondria-rich ionocytes in the kidney tubules, high renal Na⁺, K⁺-ATPase activity, and very high tissue-specific \dot{M}_{O_2} *in vitro* (Hochachka et al., 1978; Gonzalez et al., 2010; Hulbert et al., 1978a; Pelster et al., 2020b), have led these authors to suggest that the importance of the kidney relative to that of the gills for ionoregulatory homeostasis is particularly high in this species, which would be in general accord with overall trends accompanying the evolutionary transition from water-breathing to air-breathing (Smith, 1959). However, the available functional information is equivocal. With respect to the gills, both Gonzalez et al. (2010) and Pelster et al. (2020a) reported that as the animal grows, the mass-specific unidirectional Na⁺ uptake rate (active component) actually becomes larger rather than smaller, perhaps associated with the observed proliferation of ionocytes on the surface of the now finger-like gill filaments (Brauner et al., 2004; Ramos et al., 2013). The

¹Department of Zoology, University of British Columbia, Vancouver, BC, Canada V6T 1Z4. ²Department of Biology, McMaster University, Hamilton, ON, Canada L8S 4K1. ³Institute of Zoology, University of Innsbruck, Innsbruck A-6020, Austria. ⁴Center for Molecular Biosciences, University Innsbruck, Innsbruck A-6020, Austria. ⁵Laboratory of Ecophysiology and Molecular Evolution, Brazilian National Institute for Research of the Amazon, Manaus 69080-971, Brazil.

*Author for correspondence (woodcm@zoology.ubc.ca)

© C.M.W., 0000-0002-9542-2219; B.P., 0000-0002-9170-5086; S.B., 0000-0002-5594-5963; A.L.V., 0000-0002-3823-3868

List of symbols and abbreviations

ABO	air-breathing organ
$J_{X,in}$	unidirectional influx rate of substance X at the gills
$J_{X,out}$	unidirectional outflux rate of substance X at the gills
$J_{X,net}$	net flux rate of substance X at the gills
M	mass
\dot{M}_{CO_2}	carbon dioxide production rate
\dot{M}_{O_2}	oxygen consumption rate
P_{CO_2}	partial pressure of carbon dioxide
P_{O_2}	partial pressure of oxygen
P_{50}	partial pressure of oxygen at which the blood is 50% saturated
Na^+, K^+ -ATPase	sodium–potassium-activated adenosine triphosphatase
N-wastes	nitrogenous waste products
T	time
UFR	urine flow rate
Urea-N	urea nitrogen units
U_x	urinary excretion rate of substance X
V	volume
V-type H^+ -ATPase	vacuolar-type proton-activated adenosine triphosphatase

mass-specific unidirectional Na^+ efflux rate (passive component) also becomes greater in older animals, but the relative rates of efflux across the gills and via the urine from the kidney were not separated in these studies (Gonzalez et al., 2010; Pelster et al., 2020a). With respect to the kidney, spot samples of urine from both small and large *A. gigas* contained unusually low concentrations of Na^+ and Cl^- (in comparison with other teleosts) but urine flow rate was not measured, so renal ion excretion rates remain unknown (Gonzalez et al., 2010). Our second hypothesis was that the relative importance of the kidney would be greater than that of the gills in iono- and osmoregulation in pirarucu.

Hochachka et al. (1978) and Brauner et al. (2004) have suggested that the kidney plays an especially important role in N-waste excretion in pirarucu. This idea was initially based on findings of exceptionally high activity of glutamate dehydrogenase (an ammonia-producing enzyme) in the kidney, and evidence that NH_4^+ was more effective than K^+ in activating renal Na^+, K^+ -ATPase activity in adult *A. gigas* (Hochachka et al., 1978). The idea was also later supported by measurements of unusually high concentrations of ammonia in spot samples of urine (Gonzalez et al., 2010). However, renal excretion rates of N-wastes have never been reported. Therefore, our third hypothesis was that N-waste excretion through the kidney of *A. gigas* would be exceptionally high relative to that in most other teleost fish.

With these hypotheses in mind, we made long-term measurements of urine flow and renal excretion rates of Na^+, K^+, Cl^- , ammonia and urea-N in 3- to 4-month-old pirarucu, the same approximate size as the ‘large’ animals studied by both Gonzalez et al. (2010) and Pelster et al. (2020a,b). We also measured unidirectional Na^+ influx and efflux rates across the gills, and net branchial flux rates of Na^+, K^+, Cl^- , ammonia and urea-N. For the first hypothesis, experimental treatments were designed to perturb the O_2 supply to the gills and ABO separately. To address this, as well as the second and third hypotheses, simultaneous measurements of ion and N-waste fluxes at gills and kidney allowed quantitative comparisons between the two routes. Specifically, we reasoned that if kidney metabolism was dependent on O_2 uptake directly from the airspace of the ABO, then renal ion conservation would be expected to decrease with aerial

hypoxia and increase with aerial hyperoxia, reflected in reciprocal changes in urinary ion excretion rates. Furthermore, renal ammonia-N and urea-N excretion rates would be expected to decrease with aerial hypoxia and increase with aerial hyperoxia. We also reasoned that aquatic hypoxia and aquatic hyperoxia would be expected to perturb gill flux rates if the traditional osmoregulatory compromise applied. This concept argues that there is a trade-off between the needs for ionoregulation and the needs for respiratory gas exchange at the gills (Randall et al., 1972; Iftikar et al., 2010).

However, the situation is complicated by reports (Wood et al., 2007, 2009; De Boeck et al., 2013; Robertson et al., 2015) that several water-breathing, very hypoxia-tolerant Amazonian teleosts, including the oscar (*Astronotus ocellatus*) and the tambaqui (*Colossoma macropomum*), do not exhibit the traditional osmoregulatory compromise of increased flux rates during hypoxia. Rather they decrease ion fluxes and N-waste excretion rates across the gills during aquatic hypoxia by selective reductions in branchial permeability, without apparently compromising the capacity for O_2 uptake. Most importantly, a facultative air-breathing Amazonian teleost, the jeju (*Hoplerhythrinus unitaeniatus*) was able to simply avoid the gill-perturbing effects of both aquatic hypoxia and aquatic hyperoxia by resorting to air-breathing (Wood et al., 2016). Therefore, our fourth and final hypothesis was that *A. gigas* would be able to avoid the symptoms of the osmoregulatory compromise at the gills during aquatic and aerial hypoxia and hyperoxia.

MATERIALS AND METHODS**Experimental animals**

Measurements were performed on 26 pirarucu [*Arapaima gigas* (Schinz 1822); 450–900 g, sex unknown, approximately 3–4 months old] at the Laboratory of Ecophysiology and Molecular Evolution (LEEM) of the Brazilian National Institute for Research of the Amazon (INPA). The fish were obtained from local commercial aquaculture in Manaus. At INPA, they were held in large shaded outdoor tanks with free access to air, and fed daily with commercial pellets (NutripeixeTr36, Purina, São Paulo, Brazil; 36% protein). The composition of the well water, which was also used in all experiments, was ($\mu\text{mol l}^{-1}$): 200–250 Na^+ , 10–20 K^+ , 3–5 Ca^{2+} , 3–8 Mg^{2+} and 150–200 Cl^- ; pH 6.0–6.5. The acclimation and experimental temperatures were 27–29°C. The fish were fasted for 2–7 days prior to all experiments. For blood sampling and urinary cannulation, light anaesthesia [0.05 mg l^{-1} tricaine methane sulfonate (MS-222), neutralized with NaOH to pH 6.0; Sigma-Aldrich, St Louis, MO, USA] was performed in shallow tanks (4 cm depth), taking care to keep the mouth above water so that the fish did not drown in the process. As soon as the fish became unresponsive, it was transferred to a V-board in air for blood sampling or cannulation. For terminal sampling and euthanasia, lethal anaesthesia was used (0.5 mg l^{-1} MS-222, neutralized to pH 6.0, followed by a cranial concussion). All protocols were in compliance with Brazilian national and INPA animal care regulations (protocol 04/2018, SEI 1280.000209/2018-74).

Blood sampling

Blood samples (0.5 ml) were drawn by caudal puncture from eight lightly anaesthetized pirarucu into syringes pre-rinsed with lithium heparin ($1000 \text{ i.u. ml}^{-1}$; Sigma-Aldrich) in Cortland saline (Wolf, 1963). The blood was immediately centrifuged (2 min, 5000 g). The plasma was decanted, frozen in liquid N_2 and stored at -80°C for later analyses of plasma Na^+, K^+, Cl^- , total ammonia, urea-N and total CO_2 concentrations. These fish were recovered, but not used for other experiments reported here.

Enzyme activities

Kidney and intestinal tissues were taken from seven terminally anaesthetized pirarucu for Na⁺,K⁺-ATPase and vacuolar-type (V-type) H⁺-ATPase activity measurements. These were the same 'large' fish as those sampled for gill and ABO enzyme measurements by Pelster et al. (2020b) and analytical methods for enzyme activities of Kültz and Somero (1995) were identical, so the data could be directly compared. When dissecting kidney tissues, we were careful to avoid ABO tissue, and intestinal tissue was taken by scraping the luminal surface of the anterior intestine with a glass slide to sample mainly mucosal epithelium.

Urinary cannulation

Urinary catheters were placed into 11 fish. As recommended by Wood and Patrick (1994), initial dissections of dead fish were made to determine the depth and angle at which the urinary catheter should be inserted through the urogenital papilla and into the urinary bladder. The opening of the papilla and the size of the bladder are both relatively small in this species. Depending on the size of the fish, urinary catheters were fashioned from PE50 or PE60 tubing (Becton, Dickinson and Co., Franklin Lakes, NJ, USA), were typically 120–150 cm in length to accommodate the spontaneous movement of the animals in the experimental chambers, and were passed through a short external sleeve (5 cm) made of PE160 or PE190 tubing that had been heat-flared at both ends. Before cannulation, the catheter was lightly heat-polished at the tip, marked for depth, and filled with deionized water.

The anaesthetized pirarucu was placed ventral-side up on a V-board in air. With practice, the catheter could be placed in about 5 min, so it was not necessary to provide artificial ventilation of the ABO. The catheter was inserted into the urinary bladder, and a 2-0 silk ligature (Ethicon, Somerville, NJ, USA) was tied around the urogenital papilla. The sleeve was then moved to within 0.5 cm of the papilla, glued in place with cyanoacrylate glue (Vetbond; 3M Corporation, Saint Paul, MN, USA), and anchored to the ventral surface of the fish with several 2-0 silk stitches using Ethicon pre-threaded suture needles. This prevented back and forth movement, ensuring that the catheter tip remained in the bladder. The other end of the catheter was plugged with a stainless-steel pin, and the animal was transferred to its experimental chamber. The pin was removed after about 1 h, and thereafter the urine was continuously collected by a siphon about 10 cm below the water surface into a covered vessel. As explained by Wood and Patrick (1994), this technique collects ureteral urine, because it is removed from the bladder as soon as it is formed. We found that urine flow was unaffected by varying the siphon height below the water surface from 1 to 10 cm (the latter was convenient), but stopped if the catheter was raised above the water surface. Urine flow rate (UFR) was continuously monitored over 1–2 days of recovery before experiments started. There was a slight positive correlation ($r=0.33$, $N=11$) between UFR and body mass which was not statistically significant ($P=0.16$), and the range of body mass (less than 2-fold) was not sufficient to calculate a meaningful scaling coefficient, so UFR values were simply divided by body mass.

Experimental chambers and treatments

Two-chambered respirometers similar to those of Stevens and Holeton (1978) were used. The air chamber where the fish surfaced to breathe had a capacity of 0.32 liters, and the water chamber had a capacity of 8 liters. Plastic-wrapped bricks were placed in the water chamber to confine the fish to one side and prevent it from turning around. These also decreased the water volume to about 4 liters to

increase resolution in flux measurements. The exact water volume was measured at the end of the trials when the fish was euthanized by overdose of neutralized MS-222 (0.5 g l⁻¹) and removed from the chamber. Oxygen partial pressures in water and air were monitored throughout the experiments using a hand-held Accumet meter and polarographic electrode (Fisher Scientific, Toronto, ON, Canada).

Experiments typically started at 09:00 h and ended at 18:00 h, in an outdoor laboratory illuminated with diffuse daylight. One hour prior to the start of each experiment the water was changed by carefully siphoning out 80% of the volume and replacing it three times, with the final fill back to a constant-volume line. This was done again after the end of each experiment, prior to the overnight dark period. Water samples (2×5 ml) were taken prior to and immediately after each water change for ²²Na counting, to keep track of the radioactivity contained within the fish (see below). Collection of urine flow continued overnight prior to the next experiment to provide a large volume sample and ensure continued patency of the urinary catheter. The 11 fish were used in 29 separate experiments. As there were four experimental treatments, each fish was used in two to four different treatments presented in random order on different days.

Each experiment lasted 9 h and consisted of an initial normoxic control period (3×1 h) with normoxia in both aquatic and air phases, an experimental treatment period (3×1 h), and a normoxic recovery period (3×1 h). All urinary parameters and most branchial parameters were measured on an hourly basis, whereas two of the latter (urea-N and Cl⁻ net flux rates) were measured only over 3 h periods as there were insufficient changes in water composition over 1 h for adequate resolution. During normoxic control and normoxic recovery periods, as well as overnight periods, the water was continuously aerated and the air chamber was continuously flushed with room air by a high-volume air pump.

During aerial hypoxia (aquatic normoxia) treatments ($N=8$), the air chamber was flushed with a 75% air and 25% nitrogen mixture provided by a gas-mixing pump (SA27/2, Wösthoff Messtechnik, Bochum, Germany). This 75% air saturation created an air P_{O_2} of about 115 Torr or 15.3 kPa. This aerial hypoxia level was chosen because we found in our earlier studies that if P_{O_2} were lowered below about 70% air saturation, struggling ensued (Pelster et al., 2020a). Periodic air bubbling ensured that the water P_{O_2} stayed at 80–100% air saturation, so the fish was exposed to aerial hypoxia but waterborne normoxia.

During aerial hyperoxia (aquatic normoxia) treatments ($N=5$), the air chamber was continually flushed with a 50% O₂ and 50% air mixture provided by the gas-mixing pump. Theoretically this should have created an air phase P_{O_2} over 300% air saturation, but as our meter could only measure up to 200% air saturation, it is reported as >200% air saturation (>306 Torr, >40.9 kPa). The water chamber was periodically bubbled with air to keep the water P_{O_2} at 80–100% air saturation, so the fish was exposed to aerial hyperoxia but waterborne normoxia.

During aquatic hypoxia (aerial normoxia) treatments ($N=9$), the water chamber was bubbled with nitrogen, which was periodically turned on and off to maintain a water phase P_{O_2} of about 20% saturation (31 Torr, 4.1 kPa; range 10–30%). At the same time, the air chamber was flushed with room air by the high-volume air pump, so the fish was exposed to waterborne hypoxia but aerial normoxia.

During aquatic hyperoxia (aerial normoxia) treatments ($N=7$), the water chamber was bubbled with O₂, which was periodically turned on and off to maintain a water phase P_{O_2} of >200% saturation

(>306 Torr, >40.9 kPa). At the same time, the air chamber was flushed with room air by the high-volume air pump, so the fish was exposed to waterborne hyperoxia but aerial normoxia.

Measurements of renal and branchial ion fluxes and nitrogen excretion rates

Urine flow rate (UFR) was measured gravimetrically by timed collection over each 1 h interval, as well as for the overnight periods, and was expressed on a body mass basis ($\text{ml kg}^{-1} \text{h}^{-1}$). These samples were immediately frozen at -20°C , and later analysed for Na^+ , K^+ , Cl^- , ammonia and urea-N concentrations ($[\text{X}]_u$, in $\mu\text{mol ml}^{-1}$). Additionally, the overnight collections were analysed for total CO_2 because there would be less chance of CO_2 loss from these high-volume collections. Urinary excretion rates of each component (U_X , in $\mu\text{mol kg}^{-1} \text{h}^{-1}$) were calculated as:

$$U_X = [\text{X}]_u \times \text{UFR}. \quad (1)$$

As urine flow was collected externally, the assumption was made in the usual manner that fluxes measured by monitoring changes in the composition of the water phase were of branchial origin, as described by Wood (1992). In the water phase, unidirectional branchial flux rates ($J_{\text{Na},\text{in}}$, $J_{\text{Na},\text{out}}$) and net flux rates ($J_{\text{Na},\text{net}}$) of Na^+ , as well as net flux rates of ammonia ($J_{\text{amm},\text{net}}$) and K^+ ($J_{\text{K},\text{net}}$) were measured over 1 h periods, whereas net flux rates of urea-N ($J_{\text{urea-N},\text{net}}$) and chloride ($J_{\text{Cl},\text{net}}$) were measured over 3 h periods.

At the start of each experiment, 4–6 μCi (148–222 kBq) of radioactive ^{22}Na (as NaCl ; New England Nuclear Dupont, Boston, MA, USA, supplied by REM, Sao Paulo, Brazil) was added to the water phase, allowed to mix for 15 min, and then water samples were taken at 0 h and hourly intervals thereafter up to 9 h, for measurements of radioactivity ($2 \times 5 \text{ ml}$) and ion plus N-waste concentrations (20 ml).

Net flux rates of a substance X ($J_{X,\text{net}}$, in $\mu\text{mol kg}^{-1} \text{h}^{-1}$) were calculated as:

$$\frac{J_{X,\text{net}} = ([\text{X}]_i - [\text{X}]_f) \times V}{T \times M}, \quad (2)$$

where $[\text{X}]_i$ and $[\text{X}]_f$ are respectively the initial and final concentrations of X ($\mu\text{mol l}^{-1}$) in the water, V is the initial external water volume (liters), T is time period (h) and M is body mass (kg). By convention, positive values represent net uptake by the fish, while negative values represent net losses from the fish.

Unidirectional Na^+ influx rate at the gills ($J_{\text{Na},\text{in}}$, positive, in $\mu\text{mol kg}^{-1} \text{h}^{-1}$) was measured by monitoring the disappearance of ^{22}Na from the water into the fish:

$$J_{\text{Na},\text{in}} = \frac{([\text{R}]_i - [\text{R}]_f) \times V - \text{SA}_{\text{int}} \times ([\text{Na}]_i - [\text{Na}]_f)}{(\text{SA}_{\text{ext}} - \text{SA}_{\text{int}}) \times T \times M}, \quad (3)$$

where $[\text{R}]_i$ is the initial radioactivity in the water (in cpm l^{-1}) at the start of the flux period, $[\text{R}]_f$ is the final radioactivity in the water (in cpm l^{-1}) at the end of the flux period, $[\text{Na}]_i$ and $[\text{Na}]_f$ are the initial and final concentrations of total Na^+ in the water (in $\mu\text{mol l}^{-1}$), respectively, SA_{ext} is the mean external specific activity (radioactivity per total Na^+) in the water (in $\text{cpm } \mu\text{mol}^{-1}$; calculated from measurements of water radioactivity and total water $[\text{Na}^+]$ at the start and end of the flux period), SA_{int} is the mean internal specific activity in the fish (in $\text{cpm } \mu\text{mol}^{-1}$), and V (in liters), T (in h) and M (in kg) are as defined above. This equation, originally derived by Maetz (1956), incorporates correction for backflux of radioactivity from the fish to

the water as SA_{int} increases over time. As noted earlier, it was therefore important to keep track of the radioactivity in each fish to allow calculation of SA_{int} at each time.

Unidirectional Na^+ efflux rate at the gills ($J_{\text{Na},\text{out}}$, negative, in $\mu\text{mol kg}^{-1} \text{h}^{-1}$) was calculated by difference:

$$J_{\text{Na},\text{out}} = J_{\text{Na},\text{net}} - J_{\text{Na},\text{in}}. \quad (4)$$

Analytical techniques

Total ammonia concentrations in water and urine, and urea-N concentrations in water, urine and plasma, were determined by the colorimetric methods of Rahmatullah and Boyde (1980) and Verdouw et al. (1978), respectively. Particularly high precision was required to detect small changes in water urea-N, so these assays were read in 1 cm cuvettes rather than in microplates, with closely bracketing standards. Total ammonia concentrations in plasma were measured using a commercial enzymatic assay (Raichem ammonia kit, Cliniqua Corporation, San Marcos, CA, USA) calibrated with the same standards as used for water ammonia. Total CO_2 in plasma was measured with a Corning 965 Analyser (Ciba-Corning, Halstead, Essex, UK). Concentrations of Na^+ and K^+ in water, plasma and urine were measured with a 910 Digital Flame Photometer (Instrumentação Analítica, São Paulo, Brazil), while Cl^- concentrations in water, plasma and urine were measured by the colorimetric method of Zall et al. (1956). The radioactivity of ^{22}Na in each 5 ml water sample was determined by mixing with 10 ml of Ultima Gold scintillation fluid (Perkin-Elmer, Waltham, MA, USA), then counting on a Triathler portable counter (Hidex, Helsinki, Finland). Tests showed that quench was constant, so correction was unnecessary.

Statistics

Data are expressed as means \pm s.e.m. (N), where N represents the number of animals contributing to each mean. A repeated-measures experimental design was used throughout, so a repeated-measures ANOVA approach was applied, in two different ways. First, mean overall values for each fish were compiled for the three 1 h control intervals together, the three 1 h treatment intervals together, and the three 1 h recovery intervals together. Then a repeated-measures ANOVA was applied to evaluate whether there were significant differences among the three 3 h periods (control, treatment, recovery), and if present, these were identified by Tukey's or Holm-Šidák *post hoc* test. A second approach was applied to identify whether there were significant differences from the control mean for each 1 h treatment and 1 h recovery interval; these may have been missed in the 3 h averages. This was accomplished by first testing whether there were significant differences among the three 1 h control intervals, and as there were none, the one-way ANOVA was run again, using the mean control value but individual 1 h treatment and 1 h recovery values for fish with *post hoc* testing by Dunnett's test. Repeated-measures ANOVA was also used to assess differences among tissues in enzyme activities. When data failed normality and/or homogeneity of variance tests, standard transformations (log, square root, inverse) were applied. In those cases where transformation was unsuccessful, non-parametric Friedman's repeated-measures ANOVA on ranks was employed, followed by Tukey's test. Student's paired two-tailed *t*-test was used to assess differences in flux rates between gills and kidney, or between plasma and urine. A Pearson's correlation matrix was used to evaluate relationships amongst various components of either plasma composition or urine composition. Throughout, significance was accepted for $P < 0.05$.

RESULTS

Basic ionoregulatory physiology of *A. gigas*

Na^+ , K^+ -ATPase and V-type H^+ -ATPase activities in the kidney were 10- and 2.6-fold higher, respectively, than in the gills, whereas activities of both enzymes in the intestinal epithelium were intermediate, and lowest in the ABO (Table 1). The activity of V-type H^+ -ATPase exceeded that of Na^+ , K^+ -ATPase in all tissues except the kidney, where they were about equal.

In the blood plasma, there was a remarkable discrepancy between high Na^+ and low Cl^- concentrations, with $[\text{Cl}^-]_p$ amounting to only 41% of $[\text{Na}^+]_p$ (Table 2). A fairly typical K^+ concentration contributed further to the [cation–anion] gap, which was $\sim 100 \text{ mmol l}^{-1}$. While $[\text{total CO}_2]_p$ (consisting almost entirely of $[\text{HCO}_3^-]_p$) was relatively high, it accounted for less than one-third of the discrepancy. Plasma urea-N concentrations were about 6-fold higher than ammonia concentrations (Table 2).

Urine composition measurements, made on the collections during the overnight dark period, revealed exceptionally low Na^+ , Cl^- and K^+ concentrations (Table 2). As illustrated by the [urine]:[plasma] ratios, these amounted to less than 0.3% of plasma levels for Na^+ and Cl^- , and less than 2% of plasma levels for K^+ , despite a relatively high UFR of about $10 \text{ ml kg}^{-1} \text{ h}^{-1}$, providing evidence for very strong net reabsorptive processes for these ions. However urinary [urea-N]_u and [total CO_2]_u were much less strongly reabsorbed, amounting to about 12 and 22%, respectively, of plasma levels. In marked contrast, urinary [total ammonia]_u was about 20-fold greater than the plasma concentration, indicative of strong secretion.

All these urinary parameters, except total CO_2 , were measured during the daytime experiments, and Table S1 summarizes the concentration and UFR measurements made during the control periods. There were no significant differences from any of the overnight data (cf. Table 2).

Pearson matrix analysis of plasma parameters revealed only one significant correlation, a negative relationship ($r = -0.738$, $P < 0.05$, $N = 8$) between $[\text{total CO}_2]_p$, which was at the mmol l^{-1} level, and $[\text{total ammonia}]_p$, which was at the $\mu\text{mol l}^{-1}$ level (Table S2A). In contrast, when the same analysis was applied to urinary parameters (Table S2B), there was a strong positive correlation ($r = 0.644$, $P < 0.0002$, $N = 28$) between $[\text{total CO}_2]_u$ and $[\text{total ammonia}]_u$ in urine, both of which were at the mmol l^{-1} level (Fig. 1). Although the relationship was linear with a slope (0.92) close to 1.0, on a paired basis $[\text{total ammonia}]_u$ was significantly greater than $[\text{total CO}_2]_u$ by 3.4 mmol l^{-1} (intercept). Both urinary $[\text{total CO}_2]_u$ ($r = 0.728$, $P < 0.001$, $N = 28$) and urinary $[\text{total ammonia}]_u$ ($r = 0.400$, $P < 0.05$, $N = 28$) were positively correlated with urinary $[\text{K}^+]_u$, and urinary $[\text{K}^+]_u$ was positively correlated with urinary $[\text{Na}^+]_u$ ($r = 0.506$, $P < 0.01$, $N = 28$). Notably, there was no significant correlation between UFR and any urinary concentration parameter (Table S2B).

Table 1. Activities of Na^+ , K^+ -ATPase and V-type H^+ -ATPase in the kidney, intestinal epithelium, gills and air breathing organ of *Arapaima gigas*

	Na^+ , K^+ -ATPase	V-type H^+ -ATPase
Kidney	1.706 ± 0.310^a	1.708 ± 0.310^c
Intestinal epithelium	$0.718 \pm 0.197^{a,b}$	$1.233 \pm 0.181^{c,d}$
Gills*	0.167 ± 0.038^b	0.649 ± 0.049^d
ABO*	0.088 ± 0.035^b	0.149 ± 0.043^e

Within an enzyme, means not sharing the same lowercase letter are significantly different ($P < 0.05$). Values are means \pm s.e.m. ($N = 7$); units are $\mu\text{mol ATP mg protein}^{-1} \text{ h}^{-1}$. *Data previously reported for these same fish by Pelster et al. (2020a). ABO, air-breathing organ.

Table 2. Plasma and urine composition, urine flow rate and [urine]:[plasma] ratio of *A. gigas*

	Plasma ($N = 8$)	Urine ($N = 28$ overnight collections on 11 animals)	[Urine]: [plasma]
$[\text{Na}^+]$ (mmol l^{-1})	161.91 ± 2.31	$0.25 \pm 0.06^*$	0.0015
$[\text{K}^+]$ (mmol l^{-1})	4.52 ± 0.19	$0.09 \pm 0.01^*$	0.0199
$[\text{Cl}^-]$ (mmol l^{-1})	66.13 ± 4.91	$0.18 \pm 0.03^*$	0.0027
[Total ammonia] (mmol l^{-1})	0.58 ± 0.09	$9.81 \pm 1.52^*$	16.92
[Urea-N] (mmol l^{-1})	3.39 ± 0.25	$0.40 \pm 0.11^*$	0.1179
[Total CO_2] (mmol l^{-1})	31.58 ± 0.88	$6.98 \pm 1.07^*$	0.2210
Urine flow rate ($\text{ml kg}^{-1} \text{ h}^{-1}$)	–	10.15 ± 1.04	–

* $P < 0.05$ relative to the plasma concentration. Values are means \pm s.e.m.

Table 3 summarizes branchial and renal flux rates of ions, total ammonia and urea-N measured simultaneously in the same fish during the daylight control periods. At the gills, the fish were in net Na^+ balance, with unidirectional Na^+ influx ($J_{\text{Na},\text{in}}$) and efflux rates ($J_{\text{Na},\text{out}}$) that were essentially equal, so that the branchial net flux rate ($J_{\text{Na},\text{net}}$) was not significantly different from zero, or from the very low net loss rate of Na^+ through the urine (U_{Na}). Notably, U_{Na} was only about 1% of the unidirectional Na^+ loss rate at the gills ($J_{\text{Na},\text{out}}$). However, the fish were not in net K^+ or Cl^- balance at the gills, with $J_{\text{K},\text{net}}$ and $J_{\text{Cl},\text{net}}$ rates being 20- to 40-fold greater than the very low net loss rates (U_{K} , U_{Cl}) via the urine. However, the kidney did make an important contribution to N-waste excretion with rates of U_{amm} and $U_{\text{urea-N}}$ amounting to 27–32% of the respective rates across the gills ($J_{\text{amm},\text{net}}$, $J_{\text{urea-N},\text{net}}$), and accounting for 21% (ammonia) and 24% (urea-N) of the whole animal excretion rates. Notably, ammonia excretion greatly predominated over urea-N excretion through both routes, accounting for approximately 95% of total N excretion (Table 3).

Renal responses to aerial and aquatic hypoxia and hyperoxia

In general, kidney function was largely unresponsive to experimental manipulations of the O_2 composition of either the air or water phases. Urinary composition of ions and N-wastes (Table S3A–D) and UFR and urinary excretion rates of these same substances (Figs S1–S3; Table S3E–H) remained generally

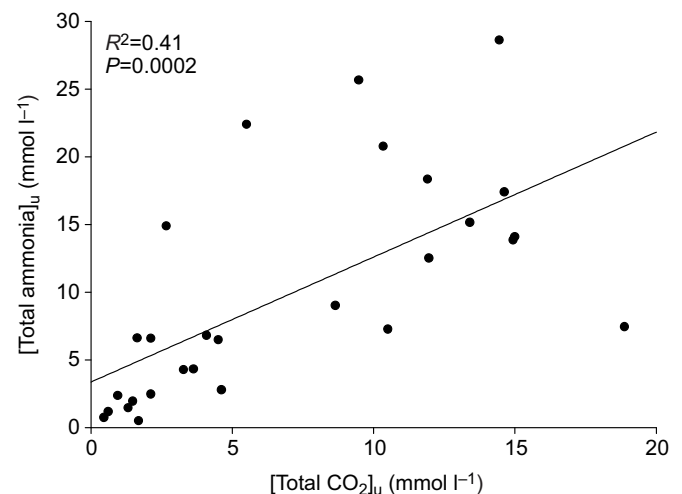


Fig. 1. The relationship between the total CO_2 concentration and total ammonia in the urine of *Arapaima gigas*, based on 28 overnight collections from 11 animals. The equation of the regression equation was: $[\text{total CO}_2]_u = 0.92[\text{total ammonia}]_u + 3.37$ ($r = 0.644$, $P < 0.0002$).

Table 3. A comparison of simultaneously measured branchial and renal flux rates of ions, total ammonia and urea-N in *A. gigas* under control conditions

	Gills	Kidney
Na ⁺ influx rate ($J_{Na,in}$, $\mu\text{mol kg}^{-1} \text{h}^{-1}$)	+214.88±15.08	–
Na ⁺ efflux rate ($J_{Na,out}$, $\mu\text{mol kg}^{-1} \text{h}^{-1}$)	–205.69±21.42	–
Na ⁺ net flux rate ($J_{Na,net}$, U_{Na} , $\mu\text{mol kg}^{-1} \text{h}^{-1}$)	+9.18±10.98	–2.74±0.75
K ⁺ net flux rate ($J_{K,net}$, U_K , $\mu\text{mol kg}^{-1} \text{h}^{-1}$)	–30.96±2.61	–1.08±0.18*
Cl [–] net flux rate ($J_{Cl,net}$, U_{Cl} , $\mu\text{mol kg}^{-1} \text{h}^{-1}$)	–42.00±15.88	–1.90±0.29*
Total ammonia net flux rate ($J_{amm,net}$, U_{amm} , $\mu\text{mol kg}^{-1} \text{h}^{-1}$)	–433.40±33.06	–116.01±17.04*
Urea-N net flux rate ($J_{urea-N,net}$, U_{urea-N} , $\mu\text{mol kg}^{-1} \text{h}^{-1}$)	–21.16±2.77	–6.79±1.58*

Values are means±s.e.m. ($N=29$ measurements on 11 animals). * $P<0.05$ relative to the rate at the gills.

unchanged during aerial hypoxia, aerial hyperoxia and waterborne hyperoxia. Exceptions included significant falls in $[\text{Na}^+]_{\text{u}}$ and U_{Na} during and after aerial hypoxia (Table S3A,E) and in U_{Na} during recovery from aerial hyperoxia (Table S3F).

The most marked exception was the renal response to aquatic hypoxia, where both the UFR (Fig. 2A) and U_{amm} (Fig. 2B) declined by 40–50% in the first hour of low waterborne P_{O_2} , but

recovered thereafter. U_K also declined, and this continued into the recovery period (Table S3G). The change in U_{amm} was driven by the decline in UFR; there was no significant change in $[\text{total ammonia}]_{\text{u}}$, although it tended to fall non-significantly, while $[\text{K}^+]_{\text{u}}$ fell significantly (Table S3C). The concentrations of the other measured components of urine composition tended to rise non-significantly (Table S3C), so renal excretion rates of all substances except ammonia remained unchanged (Table S3G).

Branchial responses to aerial and aquatic hypoxia and hyperoxia

In contrast to the kidney, gill ion transport exhibited marked responses to some of the same experimental treatments. Aerial hypoxia (aquatic normoxia) caused a 40% inhibition of $J_{\text{Na},in}$ that was significant overall, and in the second and third hours of hypoxia exposure (Fig. 3A). Furthermore, this inhibition persisted throughout the recovery period. While there was a comparable reduction in $J_{\text{Na},out}$, it was not significant during either the experimental or recovery periods, and thus there were no changes in $J_{\text{Na},net}$. There were also no significant changes in $J_{\text{K},net}$, $J_{\text{Cl},net}$, $J_{\text{urea-N},net}$ (Table 4) and $J_{\text{amm},net}$ (Fig. 3B).

Aerial hyperoxia (aquatic normoxia) also caused a 40% inhibition of $J_{\text{Na},in}$ which was significant overall, but not in any of the hourly measurements alone (Fig. 4A). During the normoxic recovery period,

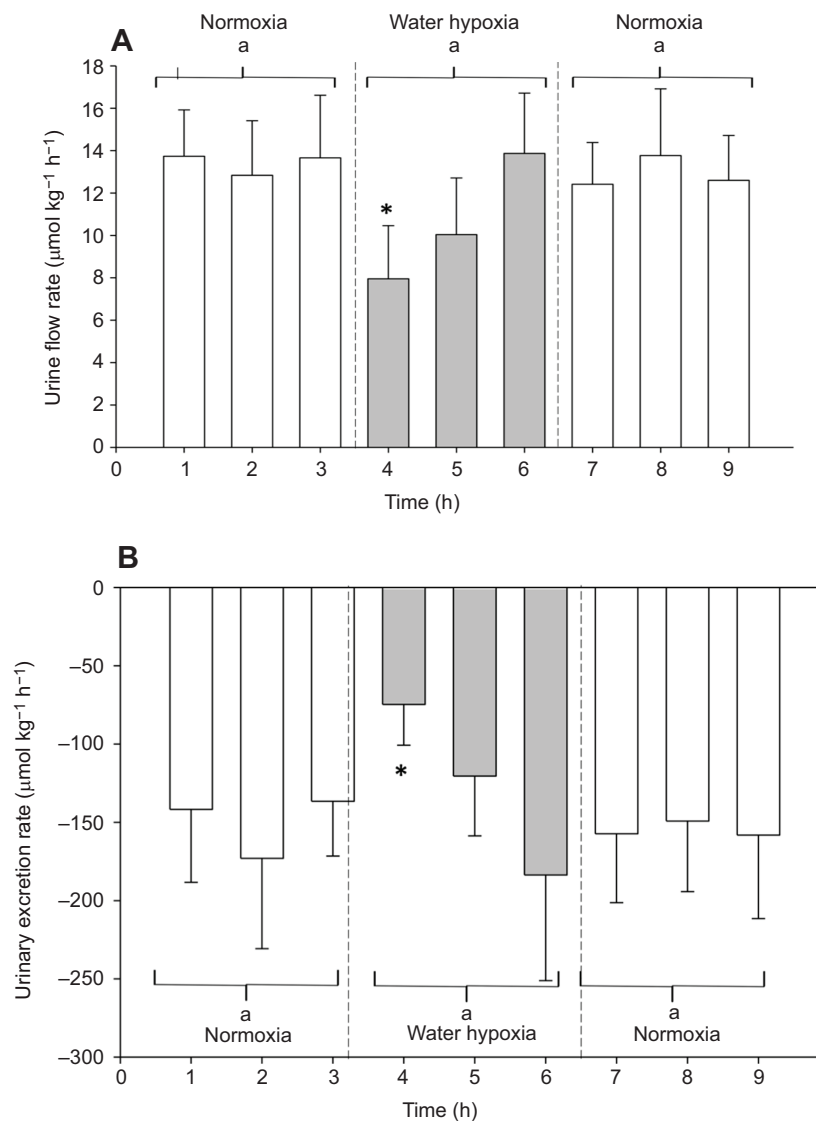


Fig. 2. Renal responses to aquatic hypoxia. The effect of aquatic hypoxia (aerial normoxia) on (A) urine flow rate and (B) urinary excretion rate of total ammonia in *A. gigas*. Aquatic hypoxia was applied during a 3 h experimental treatment period, following a 3 h normoxic control period, and was followed by a 3 h normoxic recovery period. Measurements were made over 1 h intervals. Values are means±s.e.m. ($N=9$). Overall means in 3 h periods not sharing the same lowercase letter are significantly different, and asterisks indicate means in 1 h intervals that are significantly different from the overall normoxic control mean ($P<0.05$).

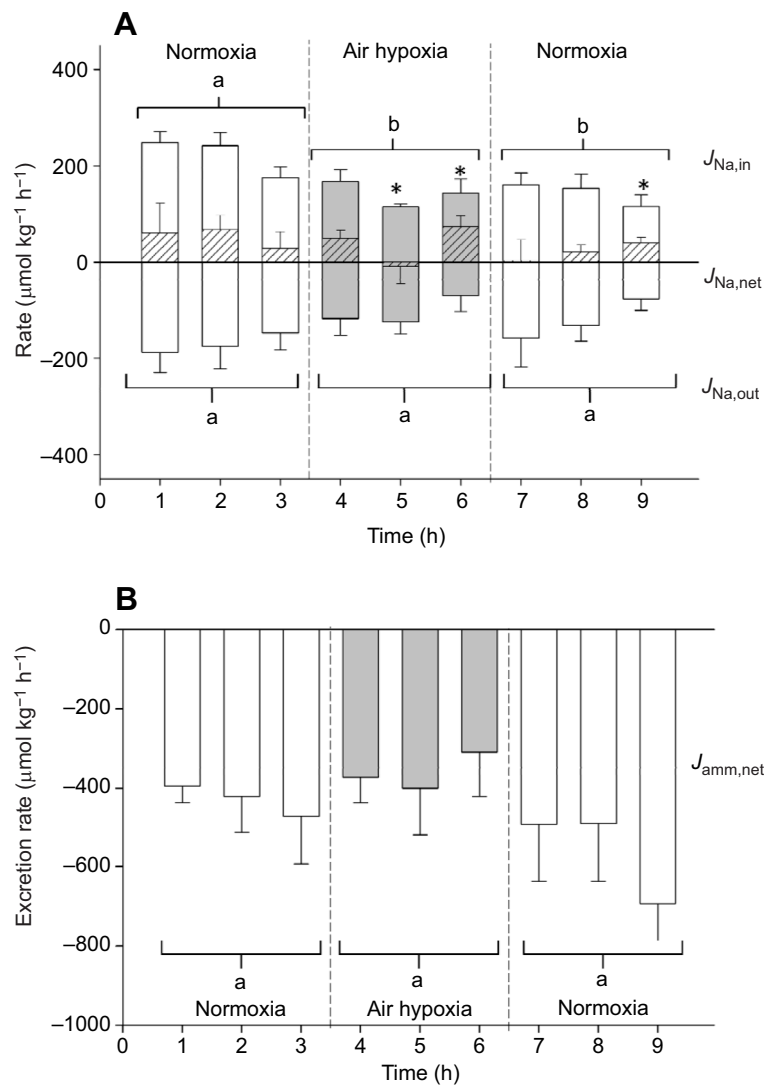


Fig. 3. Branchial responses to aerial hypoxia. The effect of aerial hypoxia (aquatic normoxia) on (A) unidirectional influx ($J_{Na,in}$), unidirectional efflux ($J_{Na,out}$) and net flux rates ($J_{Na,net}$) of Na^+ at the gills, and (B) branchial net excretion rates ($J_{amm,net}$) of total ammonia in *A. gigas*. For Na^+ fluxes, influx rates (positive) are shown as upward bars, efflux rates (negative) as downward bars, and net flux rates as hatched bars. Aerial hypoxia was applied during a 3 h experimental treatment period, following a 3 h normoxic control period, and was followed by a 3 h normoxic recovery period. Measurements were made over 1 h intervals. Values are means \pm s.e.m. ($N=9$). Overall means in 3 h periods not sharing the same lowercase letter are significantly different, and asterisks indicate means in 1 h intervals that are significantly different from the overall normoxic control mean ($P<0.05$).

there was a partial restoration of $J_{Na,in}$ so that it was no longer significantly different from the normoxic control mean. Fairly similar changes in $J_{Na,out}$ were not statistically significant. However, mean $J_{Cl,net}$ became significantly less negative during both aerial hyperoxia and recovery periods, whereas $J_{K,net}$ was less negative during the recovery period (Table 4). Both $J_{urea-N,net}$ (Table 4) and $J_{Cl,net}$ (Fig. 4B) were not affected by aerial hyperoxia or normoxic recovery.

Aquatic hypoxia (aerial normoxia) inhibited both $J_{Na,in}$ (Fig. 5A) and $J_{amm,net}$ (Fig. 5B) overall, with the most intense reductions (40–50%) in the first hour of exposure. Both parameters were restored close to control values during normoxic recovery. Although responses in $J_{Na,out}$ exhibited a similar pattern, they were not significant, and $J_{Na,net}$ remained unchanged (Fig. 5A). There were no significant alterations in $J_{K,net}$, $J_{Cl,net}$ or $J_{urea-N,net}$ (Table 4).

Aquatic hyperoxia (aerial normoxia) exerted no effects on $J_{Na,in}$, $J_{Na,out}$, $J_{Na,net}$ (Fig. 6), $J_{K,net}$ or $J_{Cl,net}$ (Table 4). However, there was a significantly elevated excretion of urea-N (more negative $J_{urea-N,net}$) during both waterborne hypoxia exposure and the subsequent normoxic recovery period (Table 4).

DISCUSSION

Overview

With respect to our original objectives, the present functional studies have revealed that *A. gigas* is equipped with a kidney that has an

exceptional capacity to produce a very high flow of urine with negligible loss of ions, and therefore plays a critical role in osmo- and ionoregulation in this species, indeed more important than that of the gills, in confirmation of our hypothesis. This finding validates the predictions of previous authors based on proxy measurements (Hochachka et al., 1978; Hulbert et al., 1978a; Gonzalez et al., 2010; Pelster et al., 2020b). We have also confirmed our hypothesis that relative to other freshwater teleosts, the pirarucu kidney makes an unusually large contribution to N-waste excretion for both ammonia and urea-N, with the former greatly predominating. This again validates ideas of previous workers (Hochachka et al., 1978; Brauner et al., 2004; Gonzalez et al., 2010). We also found evidence for a novel coupling of CO_2 excretion with ammonia excretion in the urine. However, while not definitive, the urinary data do not support our hypothesis that the transport metabolism of the kidney would depend on O_2 availability from the airspace of the surrounding ABO. There were no substantial changes in the UFR, or in the ion and N-waste concentrations in the urine, or in their excretion rates, associated with either aerial hypoxia or aerial hyperoxia. Furthermore, aquatic hypoxia and aquatic hyperoxia also had negligible effects on renal function, apart from a transient reduction of UFR and ammonia-N excretion with aquatic hypoxia. As discussed subsequently, this may have been a secondary consequence of the effects of waterborne hypoxia on gill water permeability. The most surprising findings were

Table 4. Branchial net flux rates of Cl^- , K^+ and urea-N of *A. gigas* subjected to aerial hypoxia (aquatic normoxia), aerial hyperoxia (aquatic normoxia), aquatic hypoxia (aerial normoxia) and aquatic hyperoxia (aerial normoxia) during the treatment period

	Control period	Treatment period	Recovery period
Aerial hypoxia ($N=8$)			
$J_{\text{Cl},\text{net}}$	-21.6 ± 22.16^a	-8.08 ± 7.76^a	-120.39 ± 56.63^a
$J_{\text{K},\text{net}}$	-29.69 ± 3.91^a	-28.79 ± 4.97^a	-22.81 ± 4.11^a
$J_{\text{urea-N},\text{net}}$	-24.84 ± 5.01^a	-25.72 ± 7.79^a	-21.96 ± 8.36^a
Aerial hyperoxia ($N=5$)			
$J_{\text{Cl},\text{net}}$	-49.82 ± 17.44^a	-18.74 ± 11.99^b	-16.08 ± 9.23^b
$J_{\text{K},\text{net}}$	-29.69 ± 6.19^a	$-23.36 \pm 3.82^{a,b}$	-19.50 ± 3.27^b
$J_{\text{urea-N},\text{net}}$	-22.47 ± 4.93^a	-22.61 ± 7.63^a	-18.73 ± 11.99^a
Aquatic hypoxia ($N=9$)			
$J_{\text{Cl},\text{net}}$	-74.24 ± 7.76^a	-47.21 ± 18.49^a	-29.26 ± 36.10^a
$J_{\text{K},\text{net}}$	-32.46 ± 6.40^a	-26.92 ± 3.41^a	-30.47 ± 5.14^a
$J_{\text{urea-N},\text{net}}$	-23.83 ± 4.53^a	-20.98 ± 8.84^a	-18.84 ± 7.27^a
Aquatic hyperoxia ($N=7$)			
$J_{\text{Cl},\text{net}}$	-26.97 ± 32.91^a	10.27 ± 18.04^a	-35.38 ± 18.18^a
$J_{\text{K},\text{net}}$	-31.42 ± 4.92^a	-28.38 ± 2.55^a	-21.93 ± 2.76^a
$J_{\text{urea-N},\text{net}}$	-16.28 ± 6.25^a	-31.98 ± 6.41^b	-37.1 ± 11.23^b

Values for the 3 h pre-treatment control period, 3 h treatment period and 3 h post-treatment recovery period are shown as means \pm s.e.m.; units are $\mu\text{mol kg}^{-1} \text{h}^{-1}$. Means not sharing the same lowercase letter are significantly different ($P < 0.05$) among periods for the same flux rate parameter within a particular oxygen experiment.

the marked inhibitory effects of not only aquatic hypoxia, but of also both aerial hypoxia and aerial hyperoxia on active Na^+ uptake rates ($J_{\text{Na},\text{in}}$) at the gills, thereby disproving our final hypothesis. The reduction in $J_{\text{Na},\text{in}}$ caused by waterborne hypoxia was accompanied by a reduction in branchial ammonia excretion ($J_{\text{amm},\text{net}}$), whereas aerial hypoxia and hyperoxia did not affect this parameter. The branchial responses to aquatic hypoxia fit the response pattern seen in other hypoxia-tolerant teleosts of the Amazon (Wood et al., 2007, 2009; De Boeck et al., 2013; Robertson et al., 2015). However, the effects of aerial hypoxia and hyperoxia on branchial fluxes are entirely novel, revealing unanticipated aspects of the osmoregulatory compromise.

Basic ionoregulatory physiology of *A. gigas*

The 10-fold higher levels of Na^+ , K^+ -ATPase measured in the kidney relative to the gill tissue in pirarucu (Table 1) are in qualitative agreement with previous reports (Hochachka et al., 1978; Gonzalez et al., 2010). These differences line up well with comparable differences in tissue-specific O_2 consumption rates measured in permeabilized kidney and gill cells *in vitro* (Pelster et al., 2020b). The renal Na^+ , K^+ -ATPase activity was even greater than that of the intestinal epithelium. Notably, V-type H^+ -ATPase activities were also 2.6-fold higher in kidney than in gill tissue (Table 1). These data, together with the large size and complex morphology of the kidney, and the high density of mitochondria-rich ionocytes in its tubules, are all in accordance with the high reabsorptive (Na^+ , K^+ , Cl^-) and secretory efficiencies (ammonia) of the kidney, as indicated by the urine:plasma ratios in Table 2.

Our measured concentrations of Na^+ , Cl^- , total ammonia and total CO_2 in the blood plasma (Table 2) are all in excellent agreement with those reported by Gonzalez et al. (2010) for pirarucu of similar size. However, our mean value for $[\text{urea-N}]_p$ is approximately 3-fold higher than that of Gonzalez et al. (2010); the reason for this difference is unknown, but our $[\text{urea-N}]_p$ value is very similar to that of Tavares-Dias et al. (2007). Of particular note is a very large [cation–anion] ‘gap’ calculated from $[\text{Na}^+]_p$, $[\text{K}^+]_p$ and $[\text{Cl}^-]_p$

measurements (Table 2). While $[\text{total CO}_2]_p$ (representing $[\text{HCO}_3^-]_p$) is high, a hallmark trait of fish that rely on air-breathing (Bayley et al., 2019), it accounts for only about one-third of the cation–anion gap. To our knowledge, no other teleost species exhibits such a large gap. Clearly the plasma protein must account for an unprecedented amount of negative charge, or else there must be another (unmeasured) anion. As Gonzalez et al. (2010) have pointed out, large ‘gaps’ seem to be characteristic of freshwater fish such as the eel (Farrell and Lutz, 1975; Bornancin et al., 1977; Hyde and Perry, 1989), which lack active Cl^- uptake mechanisms at the gills. In the genus *Anguilla*, the reported gap ranges from 34 (Farrell and Lutz, 1975) to 90 mequiv l^{-1} (Nakada et al., 2005) and in the latter study, SO_4^{2-} was identified as an important ‘missing anion’, contributing 38 mequiv l^{-1} . In future studies, it will be of interest to assay SO_4^{2-} levels in *A. gigas* plasma, and measure unidirectional Cl^- and SO_4^{2-} uptake at the gills.

Earlier, in the same water quality, we measured whole animal flux rates (i.e. gills and kidney combined) in pirarucu of the same size that had not been fitted with urinary catheters (Pelster et al., 2020a). For all parameters (unidirectional and net Na^+ flux rates, and net flux rates of other ions, ammonia and urea-N), there were no significant differences from the sum of branchial and renal flux rates measured separately in the present study (Table 3). From this we conclude that the presence of the catheters did not disturb the ionoregulatory or N-waste physiology of the fish.

UFR in pirarucu was exceptionally high, averaging about 10–12 $\text{ml kg}^{-1} \text{h}^{-1}$ during both daytime (Table S1, when there was activity in the laboratory) and night-time (Table 2, when there was little activity). Urinary composition, as well as ion and N-waste excretion rates, also remained constant between day- and night-time (Table S1; Tables 2 and 3). These flow rates are 3- to 5-fold higher than standard resting UFR values in most other freshwater species, based on extensive tabulations in reviews (Hickman and Trump, 1969; Wood and Patrick, 1994; Wood, 1995). Initially we suspected post-operative stress-induced ‘laboratory diuresis’ (Hunn and Willford, 1970; Wood and Patrick, 1994), but in fact rates were generally lowest in the first 6 h after cannulation, and thereafter increased to a constant level. Furthermore, two fish continued to produce at this rate for 11 days. We are aware of only one previous measurement of UFR in *A. gigas* (Brauner and Val, 1996); this was also fairly high (5.8 $\text{ml kg}^{-1} \text{h}^{-1}$), especially in light of a 2-fold greater mean body size. A more probable explanation is that these high UFRs are simply characteristic of Amazonian teleosts, as supported by similarly high resting UFRs of 10.6 $\text{ml kg}^{-1} \text{h}^{-1}$ in the catfish, *Lipossarcus* spp. (Randall et al., 1996) and 11.5 $\text{ml kg}^{-1} \text{h}^{-1}$ in the tambaqui, *C. macropomum* (Wood et al., 2017). Both the low water $[\text{Ca}^{2+}]$ (Hunn, 1985; McDonald and Rogano, 1986) and the high temperature (Mackay and Beatty, 1968) of Amazonian waters acting to increase gill water permeability and consequent urine production may be contributory factors. However, resting UFRs were much lower ($\sim 3.0 \text{ ml kg}^{-1} \text{h}^{-1}$) in the Amazonian jeju *H. unitaeniatus*, traira *Hoplias malabaricus* (Cameron and Wood, 1978) and oscar *A. ocellatus* (Wood et al., 2009) so the pattern is certainly not universal.

Regardless of the explanation, the urinary inorganic ion concentrations accompanying these high UFRs (Table 2) were lower than ever previously reported in any other teleost fish, by at least 10-fold. However, they agreed well with $[\text{Na}^+]_u$ and $[\text{Cl}^-]_u$ measurements on spot samples taken from the urinary bladder of *A. gigas* by Gonzalez et al. (2010). Again, for extensive tabulations on other species, see Hickman and Trump (1969), Mangum et al. (1978), Wood and Patrick (1994) and Wood (1995). To put these data in

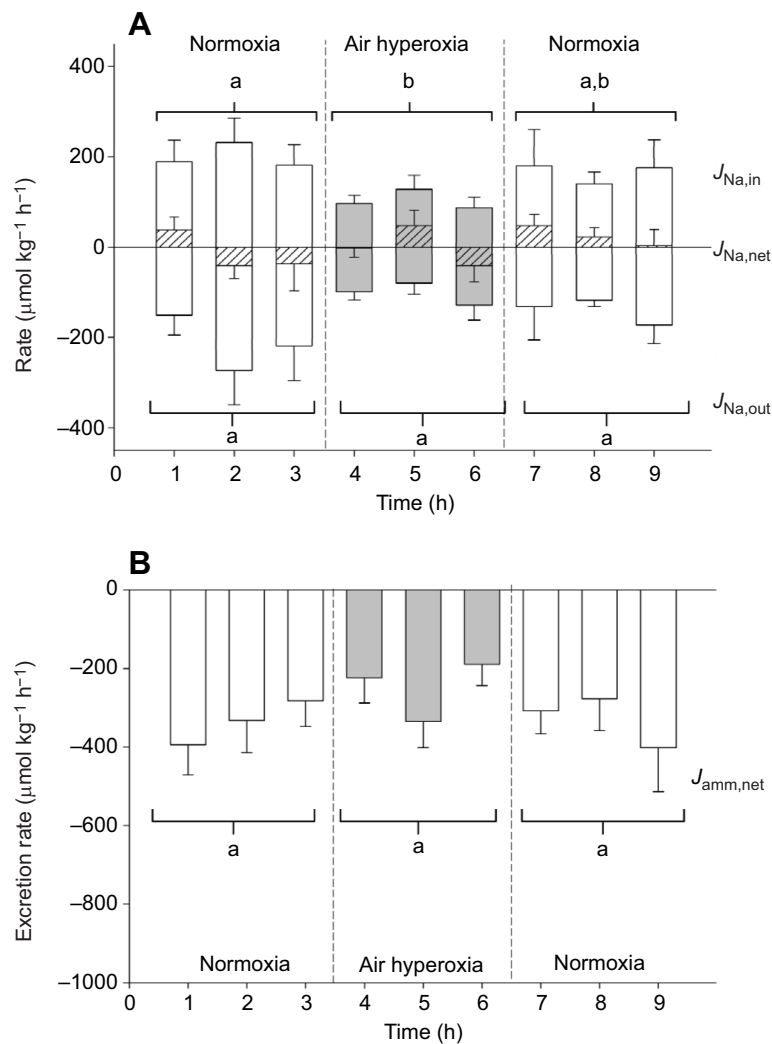


Fig. 4. Branchial responses to aerial hyperoxia. The effect of aerial hyperoxia (aquatic normoxia) on (A) unidirectional influx ($J_{Na,in}$), unidirectional efflux ($J_{Na,out}$) and net flux rates ($J_{Na,net}$) of Na^+ at the gills, and (B) branchial net excretion rates ($J_{amm,net}$) of total ammonia in *A. gigas*. For Na^+ fluxes, influx rates (positive) are shown as upward bars, efflux rates (negative) as downward bars, and net flux rates as hatched bars. Aerial hyperoxia was applied during a 3 h experimental treatment period, following a 3 h normoxic control period, and was followed by a 3 h normoxic recovery period. Measurements were made over 1 h intervals. Values are means \pm s.e.m. ($N=5$). Overall means in 3 h periods not sharing the same lowercase letter are significantly different, and asterisks indicate means in 1 h intervals that are significantly different from the overall normoxic control mean ($P<0.05$).

perspective, through their renal reabsorption abilities, pirarucu were able to bring $[Na^+]_u$ and $[Cl^-]_u$ down to levels equal to or often lower than those in the dilute water in which they were living. A conservative estimate of glomerular filtration rate (GFR) would be 1.5-fold UFR (Wood and Patrick, 1994), or about 16 ml kg⁻¹ h⁻¹. Therefore, as primary urine would contain blood plasma concentrations of Na^+ and Cl^- (Table 2), the glomerular filtration loads would be about 2600 $\mu\text{mol kg}^{-1} \text{h}^{-1}$ of Na^+ and about 1060 $\mu\text{mol kg}^{-1} \text{h}^{-1}$ of Cl^- , of which only 0.1–0.2% are excreted (Table 3), i.e. >99.8% reabsorption efficiency. At least for Na^+ , the renal reabsorption rate (2596 $\mu\text{mol kg}^{-1} \text{h}^{-1}$) would be 12-fold greater than the measured active uptake of Na^+ at the gills ($J_{Na,in}=215 \mu\text{mol kg}^{-1} \text{h}^{-1}$; Table 3), most of which is lost by diffusive efflux ($J_{Na,out}=-206 \mu\text{mol kg}^{-1} \text{h}^{-1}$; Table 3). From this simple comparison, we conclude that the kidney in fact makes a much larger contribution than the gills to ionoregulation in *A. gigas*.

Yet at the same time as the kidney scrubs the urine virtually clean of inorganic ions by reabsorptive transport, it secretes enough ammonia to raise urinary ammonia levels to 17-fold blood plasma levels, and account for 21% of whole animal ammonia excretion (Table 3). This measured urinary percentage agrees with a prediction made by Brauner et al. (2004) and is 2- to 4-fold greater than in most teleosts (reviewed by Wood, 1993), and on an absolute basis represents the highest urinary ammonia excretion rate ($\sim 116 \mu\text{mol kg}^{-1} \text{h}^{-1}$; Table 3) in any fish of which we are aware.

Although the urinary contribution to whole animal urea-N excretion is also high (24%; Table 3) relative to most other freshwater teleosts (Wood, 1993, 1995), overall urea-N excretion is a relatively small component (5%) of the overall N excretion in the pirarucu.

Mean total ammonia concentration in the urine under control conditions in *A. gigas* ($\sim 10 \text{ mmol l}^{-1}$; Table 2; Table S1) is comparable to that of trout suffering severe metabolic acidosis from environmental acid exposure (McDonald and Wood, 1981; Wood et al., 1999), yet because of the much higher UFR, U_{amm} is about 2- to 3-fold higher in the control pirarucu. Comparable low pH exposures (King and Goldstein, 1983; Wright et al., 2014; Lawrence et al., 2015) and ammonia-injection studies (Maetz, 1972) in cyprinids yielded stimulated values of $[total\ ammonia]_u$ and U_{amm} that were only a small fraction of those in control pirarucu. In *Monopterus albus*, a facultative air-breathing eel of south-east Asia, severe respiratory acidosis due to environmental hypercapnia (4 kPa) resulted in elevations of $[total\ ammonia]_u$ to comparable levels as those in control pirarucu, but U_{amm} remained much lower because of low UFR (Thin et al., 2019). In future, it will be of interest to measure U_{amm} in *A. gigas* during both environmental acid exposure and hypercapnia, both of which are common situations in the Amazon (Val and Almeida-Val, 1995; Rasera et al., 2013), as well as after normal feeding, a treatment that is known to elevate U_{amm} in other teleosts (Buckling et al., 2010; Fehsenfeld and Wood, 2018).

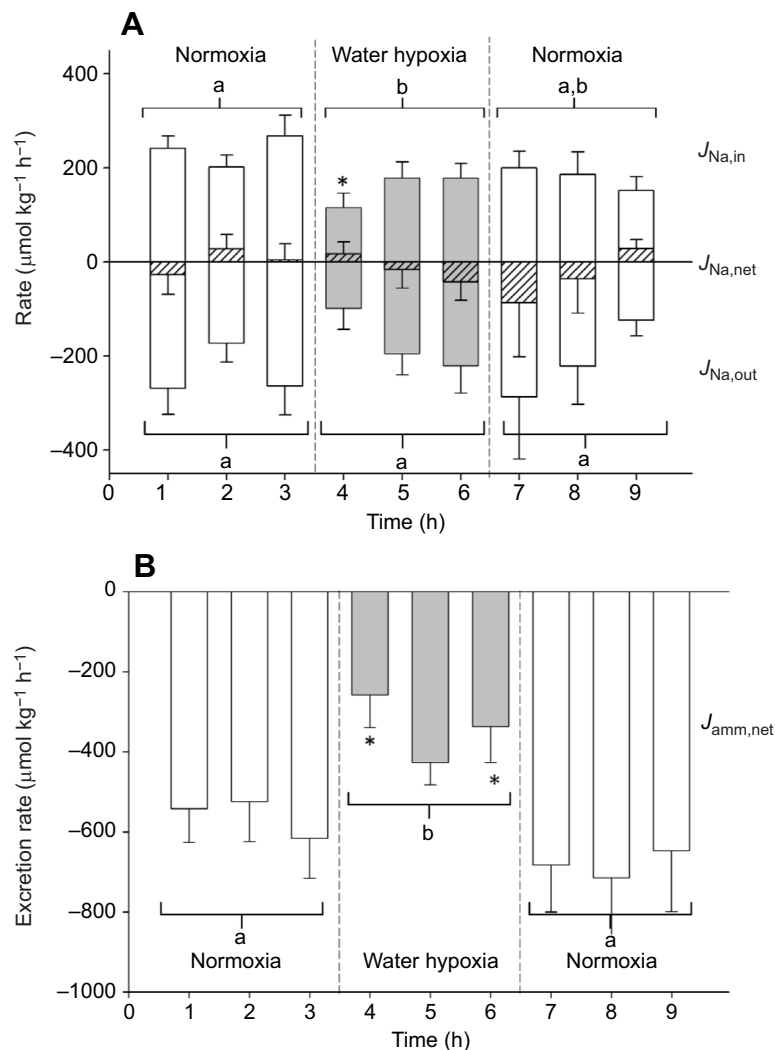


Fig. 5. Branchial responses to aquatic hypoxia. The effect of aquatic hypoxia (aerial normoxia) on (A) unidirectional influx ($J_{\text{Na},\text{in}}$), unidirectional efflux ($J_{\text{Na},\text{out}}$) and net flux rates ($J_{\text{Na},\text{net}}$) of Na^+ at the gills, and (B) branchial net excretion rates ($J_{\text{amm},\text{net}}$) of total ammonia in *A. gigas*. For Na^+ fluxes, influx rates (positive) are shown as upward bars, efflux rates (negative) as downward bars, and net flux rates as hatched bars. Aquatic hypoxia was applied during a 3 h experimental treatment period, following a 3 h normoxic control period, and was followed by a 3 h normoxic recovery period. Measurements were made over 1 h intervals. Values are means \pm s.e.m. ($N=9$). Overall means in 3 h periods not sharing the same lowercase letter are significantly different, and asterisks indicate means in 1 h intervals that are significantly different from the overall normoxic control mean ($P<0.05$).

In acid–base terms, urinary total ammonia excretion (almost entirely NH_4^+) represents acidic equivalent excretion, whereas urinary total CO_2 excretion (almost entirely HCO_3^-) represents basic equivalent excretion (see Pitts, 1963; Hills, 1973). This probably explains the reasonably tight coupling between $[\text{total CO}_2]_{\text{u}}$ and $[\text{total ammonia}]_{\text{u}}$ observed in the urine of *A. gigas* under control conditions (Fig. 1; Table S2B). The HCO_3^- excretion compensates for the NH_4^+ excretion so that there will be little net effect on the acid–base balance of the whole animal. The urine: plasma ratios (Table 2) indicate that total CO_2 , unlike total ammonia, is not secreted on a net basis, so this matching is presumably achieved by regulating the reabsorption of HCO_3^- in the renal tubules. As $[\text{total ammonia}]_{\text{p}}$ and $[\text{total CO}_2]_{\text{p}}$ in plasma are actually negatively correlated (Table S2A) and differ by more than an order of magnitude in concentration (Table 2), coupling by glomerular filtration cannot be involved. Brauner and Val (1996) reported even higher $[\text{total CO}_2]_{\text{u}}$ (mean=29 mmol l^{-1}) in the urine of resting pirarucu than in the present study ($\sim 7 \text{ mmol l}^{-1}$; Table 2), but did not measure $[\text{total ammonia}]_{\text{u}}$. Brauner and Val (1996) estimated that urinary total CO_2 excretion amounted to 6.3% of whole animal \dot{M}_{CO_2} , whereas our measurements (Table 2), in comparison with whole-animal \dot{M}_{CO_2} determined under similar conditions in pirarucu of comparable size (Pelster et al., 2020a), would yield an estimate of about 2%.

Unidirectional Na^+ influx and efflux rates at the gills were in approximate balance under control conditions (Table 3). This contrasts with the report of Gonzalez et al. (2010) where $J_{\text{Na},\text{out}}$ was approximately 3-fold higher than $J_{\text{Na},\text{in}}$ in similarly sized pirarucu. As these $J_{\text{Na},\text{out}}$ values were virtually identical to the present study, the likely explanation is the 4-fold lower water Na^+ concentration used by Gonzalez et al. (2010), which would have greatly reduced the active influx component ($J_{\text{Na},\text{in}}$) while barely affecting the diffusive loss component ($J_{\text{Na},\text{out}}$). Regardless, our measurements confirm that uptake rate is quite high in animals of this size despite the reduced gill surface area (see Introduction). Presumably, this high $J_{\text{Na},\text{in}}$ is supported by the proliferation of ionocytes on the surface of the finger-like gill filaments (Brauner et al., 2004; Ramos et al., 2013). In much smaller pirarucu, Gonzalez et al. (2010) characterized the Na^+ uptake system as one of very low capacity and low affinity; the same may not be true in larger animals. The slight negative net balance for K^+ and Cl^- at the gills (Table 3) for these fasting fish suggests that the diet normally provides an important supplement of these ions, as seen in the jeju (Wood et al., 2016).

Renal responses to aerial and aquatic hypoxia and hyperoxia
Arapaima gigas has relatively low blood O_2 affinity (i.e. high P_{50}) (Johansen et al., 1978; Randall et al., 1978). According to Randall et al. (1978), at the normal *in vivo* arterial P_{CO_2} , the P_{50} is 29.1 Torr

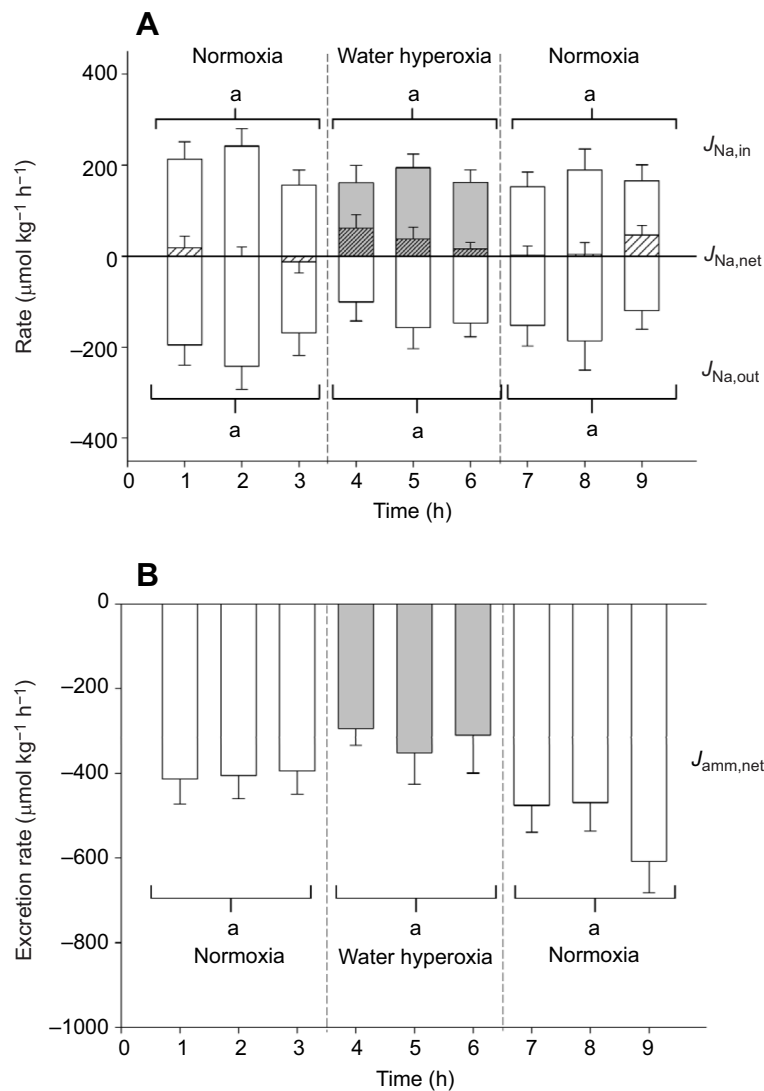


Fig. 6. Branchial responses to aquatic hyperoxia. The effect of aquatic hyperoxia (aerial normoxia) on (A) unidirectional influx ($J_{Na,in}$), unidirectional efflux ($J_{Na,out}$) and net flux rates ($J_{Na,net}$) of Na^+ at the gills, and (B) branchial net excretion rates ($J_{amm,net}$) of total ammonia in *A. gigas*. For Na^+ fluxes, influx rates (positive) are shown as upward bars, efflux rates (negative) as downward bars, and net flux rates as hatched bars. Aquatic hyperoxia was applied during a 3 h experimental treatment period, following a 3 h normoxic control period, and was followed by a 3 h normoxic recovery period. Measurements were made over 1 h intervals. Values are means \pm s.e.m. ($N=7$). Overall means in 3 h periods not sharing the same lowercase letter are significantly different, and asterisks indicate means in 1 h intervals that are significantly different from the overall normoxic control mean ($P<0.05$).

(3.9 kPa), and the measured arterial P_{O_2} is about 40 Torr (5.3 kPa), yielding an arterial saturation of only 62%, a point lying on the steep part of the blood O_2 dissociation curve. Thus if our experimental manipulations in external P_{O_2} had access to the blood, they would very likely have changed blood P_{O_2} and O_2 saturation *in vivo*.

However, contrary to our prediction that renal function would depend on direct O_2 supply from the ABO, the effects of manipulating the composition of the air phase to either 75% (15.3 kPa) or >200% (>40.9 kPa) air saturation were generally negligible on urinary flow, composition and excretion rates (Figs S1 and S2; Table S3A,B,E,F). Indeed, the reduced $[\text{Na}^+]_u$ and U_{Na} during and after aerial hypoxia (greater renal Na^+ conservation; Table S3A,E) goes directly against our prediction. The simplest explanation is that the hypothesis was incorrect, but there are several caveats. Firstly, we used only a moderate aerial hypoxia (15.3 kPa) to avoid struggling. Pelster et al. (2020a) reported that this level of hypoxia was insufficient to stimulate increased air-breathing, and would have resulted in ABO P_{O_2} values of 5–9 kPa (relative to normoxic ABO P_{O_2} values of 6–16 kPa). These may not have been low enough to impair kidney O_2 supply; for kidney cells *in vitro*, inhibited \dot{M}_{O_2} occurred at 2 kPa (Pelster et al., 2020b). Secondly, O_2 injections into the ABO have been reported to reduce the frequency of air-breathing in *A. gigas* (Farrell and Randall, 1978) so it is possible

that average ABO P_{O_2} was not greatly altered by the aerial hyperoxia treatment. Thirdly, we do not know to what extent O_2 uptake across the gills can compensate for altered O_2 supply by the ABO.

Indeed, in our system, it was not possible to measure the \dot{M}_{O_2} of the whole animal while simultaneously holding the P_{O_2} levels of the air and water phases relatively constant, so we do not know whether \dot{M}_{O_2} through either route or in total was altered. However, as the fish did not struggle, and the level of aerial hypoxia used did not alter air-breathing frequency or breath volume (Pelster et al., 2020a), we speculate that total \dot{M}_{O_2} was not greatly affected. Similarly, as we avoided blood vessel cannulation to prevent disturbance of renal function, we do not know whether the experimental treatments affected blood acid–base status, which in turn could have affected gill or kidney function. In future experiments, it will be useful to monitor \dot{M}_{O_2} from the two phases during these experimental treatments, as well as blood respiratory gases and acid–base status, and also to experimentally manipulate blood O_2 capacity and affinity. Additionally, vascular casting and histology will be useful to see if there are direct connections between ABO blood vessels and kidney vessels, and to measure diffusion distances from the ABO to renal capillaries.

Aquatic hypoxia (4.1 kPa) did affect kidney function, causing transient 40–50% decreases in both UFR (Fig. 2A) and U_{amm}

(Fig. 2B), and a longer-lasting fall in U_K (Table S3G). The fall in UFR has been seen previously in the Amazonian oscar (Wood et al., 2009) and may in fact be a consequence of a general reduction in gill permeability during aquatic hypoxia that has been reported in the oscar and in other species of hypoxia-tolerant but water-breathing fish (Wood et al., 2007, 2019; De Boeck et al., 2013; Robertson et al., 2015; Giacomini et al., 2020). Decreased permeability leads to decreased water entry, decreased GFR and decreased UFR. The decreases in U_{amm} (Fig. 2B) and U_K (Table S3G) reflect the fact that, unlike other urinary components, their urinary concentrations tended to fall during aquatic hypoxia (Table S3C). NH_4^+ and K^+ often share the same transporters or channels (e.g. Kinne et al., 1986; Yellen, 1987; Randall et al., 1999; Choe et al., 2000) and indeed their concentrations in urine were positively correlated under control conditions (Table S2B). We are aware of no previous reports on the effects of aquatic hypoxia on kidney function in an obligate air-breathing fish. However, when the marbled swamp eel (*Synbranchus marmoratus*), a facultative air-breather, was forced to rely almost exclusively on air-breathing by aquatic hypoxia (10% saturation), UFR did not change (Heisler, 1982), whereas in another swamp eel (*Monopterus albus*), UFR fell during air exposure (Thin et al., 2019).

Branchial responses to aerial and aquatic hypoxia and hyperoxia

As noted above, the branchial responses to aquatic hypoxia [significantly reduced $J_{\text{Na},\text{in}}$ and $J_{\text{amm},\text{net}}$, non-significantly reduced $J_{\text{Na},\text{out}}$ (Fig. 5), with evidence of reduced water entry provided by reduced UFR (Fig. 2A)] all fit the response pattern seen in other hypoxia-tolerant teleosts where branchial fluxes of ions, water and ammonia are decreased by selective reductions in permeability and ion transport that do not appear to affect respiratory gas exchange (Wood et al., 2007, 2009, 2019; Scott et al., 2008; Matey et al., 2011; De Boeck et al., 2013; Robertson et al., 2015; Giacomini et al., 2020). This is different from the traditional osmorepiratory compromise seen in fish that are not tolerant of hypoxia (Randall et al., 1972; Ifikar et al., 2010; Robertson et al., 2015). It is also different from the Amazonian jeju that avoids the problem by increased reliance on air-breathing (Wood et al., 2016). *Arapaima gigas* of this size source only about 25–30% of their \dot{M}_{O_2} from the water phase (Gonzalez et al., 2010; Pelster et al., 2020a), and according to Fernandes et al. (2012), ABO respiratory surface area is 2.79-fold greater, and ABO diffusing capacity for respiratory gases is 88-fold higher than those of the gills. Therefore, it is surprising that the pirarucu makes such a pronounced adjustment in gill function during waterborne hypoxia. Nevertheless, as 88–90% of \dot{M}_{CO_2} occurs to the water phase (Gonzalez et al., 2010; Pelster et al., 2020a), these fish must maintain branchial blood flow and keep ventilating their gills to wash out CO_2 to the hypoxic water. Perhaps there is a direct effect of water P_{O_2} on the branchial epithelium that proves helpful in reducing ionoregulatory costs at a time of O_2 limitation.

The effects of both aerial hypoxia and hyperoxia on branchial Na^+ fluxes were also surprising, and entirely novel, revealing aspects of the osmorepiratory compromise that would not have been anticipated based on structure alone (Ramos et al., 2013). The fact that these treatments affected only unidirectional Na^+ fluxes (Figs 3A,4A) and not branchial ammonia fluxes (Figs 3B,4B) or UFR (Figs S1A,2A), potentially indicative of branchial water uptake, all suggest that the phenomena were somewhat different from that seen during aquatic hypoxia (cf. Figs 2A,5B). An additional difference is the clear persistence of reduced $J_{\text{Na},\text{in}}$ into

the normoxic recovery period after aerial hypoxia exposure (Fig. 3A). In functional terms, it would be adaptive to reduce branchial ionoregulatory costs when O_2 availability through the major route, the ABO, is compromised by aerial hypoxia. While this is the same argument as made earlier for cost-saving during aquatic hypoxia, the explanation obviously cannot be a direct effect of air P_{O_2} on the gill epithelium. In mechanistic terms, a neurohumoral control, perhaps acting through the autonomic nervous system or circulating stress hormones (e.g. Donald, 1989; Sundin and Nilsson, 2002; Marshall, 2003; Jonz and Zaccane, 2009) may be a more likely explanation, and could account for the persistent inhibition of branchial $J_{\text{Na},\text{in}}$ during normoxic recovery. Indeed, there is precedence for such a long-lasting effect seen in a continuing reduction in gill water permeability of the freshwater killifish during 3 h of normoxic recovery after 3 h of severe aquatic hypoxia (10% air saturation; Wood et al., 2019).

It is more difficult to explain why aerial hyperoxia should inhibit branchial $J_{\text{Na},\text{in}}$ (Fig. 4A) and also branchial $J_{\text{K},\text{net}}$ and $J_{\text{Cl},\text{net}}$ (Table 4). Perhaps with reduced need for waterborne O_2 uptake, bypass shunting of blood flow through the gills and reduced water ventilation will reduce perfusion and irrigation of the ionocytes. However, this might also be expected to reduce $J_{\text{amm},\text{net}}$, yet this did not occur (Fig. 4B). Furthermore, both $J_{\text{Na},\text{in}}$ (Fig. 6A) and $J_{\text{amm},\text{net}}$ (Fig. 6B) were unaffected during aquatic hyperoxia, but $J_{\text{urea-N},\text{net}}$ was increased (Table 4). As reviewed by Pelster and Wood (2018), our understanding of the interplay between ionoregulation and respiratory gas exchange accompanying the evolution of air-breathing in fish remains fragmentary, and far more work is needed. An important recent advance is the discovery of neuroepithelial cells, putative multi-modal $\text{O}_2/\text{CO}_2/\text{pH}/\text{ammonia}$ receptors (Jonz, 2018), both in the gills and the glottis leading to the ABO in *A. gigas* (Zaccane et al., 2020). At least in water-breathing fish, neuroepithelial cells are involved in cardioventilatory control (Jonz and Zaccane, 2009; Jonz, 2018); it may not be too great a leap to predict that they may also be involved in ionoregulatory control.

Acknowledgements

We thank Dr Anne Cremazy and Dr Kevin Brix for practical help, and Dr Sunita Nadella for help with statistical analyses and graphing.

Competing interests

The authors declare no competing or financial interests.

Author contributions

Conceptualization: C.M.W., B.P., A.L.V.; Methodology: C.M.W., B.P., S.B.-M., A.L.V.; Validation: C.M.W., A.L.V.; Formal analysis: C.M.W., B.P., S.B.-M.; Investigation: C.M.W., B.P., S.B.-M.; Resources: C.M.W., B.P.; Data curation: C.M.W., B.P., S.B.-M.; Writing - original draft: C.M.W.; Writing - review & editing: B.P., A.L.V.; Visualization: C.M.W.; Supervision: C.M.W., A.L.V.; Project administration: C.M.W., A.L.V.; Funding acquisition: C.M.W., B.P., A.L.V.

Funding

Financial support by INCT ADAPTA–CNPq (465540/2014–7), Fundação de Amparo à Pesquisa do Estado do Amazonas (FAPEAM; 062.1187/2017), Coordenação de Aperfeiçoamento de Pessoal de Nível Superior (CAPES; finance code 001), Science without Borders (Brazil), and Natural Sciences and Engineering Research Council of Canada (Discovery Grant; RGPIN-2017-03843) is gratefully acknowledged. A.L.V. is the recipient of a research fellowship from Brazilian CNPq.

Supplementary information

Supplementary information available online at <https://jeb.biologists.org/lookup/doi/10.1242/jeb.232694.supplemental>

References

Bayley, M., Damsgaard, C., Thomsen, M., Malte, H. and Wang, T. (2019). Learning to air-breathe: the first steps. *Physiology* **34**, 14–29. doi:10.1152/physiol.00028.2018

- Bornancin, M., De Renzis, G. and Maetz, J.** (1977). Branchial Cl transport, anion-stimulated ATPase and acid-base balance in *Anguilla anguilla* adapted to freshwater: effects of hyperoxia. *J. Comp. Physiol.* **117**, 313-322. doi:10.1007/BF00691557
- Brauner, C. J. and Val, A. L.** (1996). The interaction between O₂ and CO₂ exchange in the obligate air-breather *Arapaima gigas*, and the facultative air breather, *Lipossarcus pardalis*. In *Physiology and Biochemistry of the Fishes of the Amazon* (ed. A. L. Val, V. Almeida-Val and D. J. Randall), pp. 101-110. Manaus, Brazil: INPA.
- Brauner, C. J., Matey, V., Wilson, J. M., Bernier, N. J. and Val, A. L.** (2004). Transition in organ function during the evolution of air-breathing; insights from *Arapaima gigas*, an obligate air-breathing teleost from the Amazon. *J. Exp. Biol.* **207**, 1433-1438. doi:10.1242/jeb.00887
- Bucking, C., Landman, M. J. and Wood, C. M.** (2010). The role of the kidney in compensating the alkaline tide, electrolyte load, and fluid balance disturbance associated with feeding in the freshwater rainbow trout. *Comp. Biochem. Physiol.* **A 156**, 74-83. doi:10.1016/j.cbpa.2009.12.021
- Cameron, J. N. and Wood, C. M.** (1978). Renal function and acid-base regulation in two Amazon erythrinid fishes: *Hoplias malabaricus*, a water breather, and *Hoplerhynchus unitaeniatus*, a facultative air breather. *Can. J. Zool.* **56**, 917-930. doi:10.1139/z78-127
- Choe, H., Sackin, H. and Palmer, L. G.** (2000). Permeation properties of inward-rectifier potassium channels and their molecular determinants. *J. Gen. Physiol.* **115**, 391-404. doi:10.1085/jgp.115.4.391
- De Boeck, G., Wood, C. M., Iftikar, F. I., Matey, V., Scott, G. R., Sloman, K. A., da Silva, M. D. N. P., Almeida-Val, V. M. F. and Val, A. L.** (2013). Interactions between hypoxia tolerance and food deprivation in Amazonian oscar, *Astronotus ocellatus*. *J. Exp. Biol.* **216**, 4590-4600. doi:10.1242/jeb.082891
- Donald, J. A.** (1989). Adrenaline and branchial nerve stimulation inhibit ⁴⁵Ca influx into the gills of rainbow trout, *Salmo gairdneri*. *J. Exp. Biol.* **141**, 441-445.
- Farrell, A. P. and Lutz, P. L.** (1975). Apparent anion imbalance in the fresh water adapted eel. *J. Comp. Physiol.* **102**, 159-166. doi:10.1007/BF00691301
- Farrell, A. P. and Randall, D. J.** (1978). Air-breathing mechanics in two Amazonian teleosts, *Arapaima gigas* and *Hoplerhynchus unitaeniatus*. *Can. J. Zool.* **56**, 939-945. doi:10.1139/z78-129
- Fehsenfeld, S. and Wood, C. M.** (2018). Section-specific expression of acid-base and ammonia transporters in the kidney tubules of the goldfish *Carassius auratus* and their responses to feeding. *Am. J. Physiol.* **315**, F1565-F1582. doi:10.1152/ajprenal.00510.2017
- Fernandes, M. N., da Cruz, A. L., da Costa, O. T. F. and Perry, S. F.** (2012). Morphometric partitioning of the respiratory surface area and diffusion capacity of the gills and swim bladder in juvenile Amazonian air-breathing fish, *Arapaima gigas*. *Micron* **43**, 961-970. doi:10.1016/j.micron.2012.03.018
- Giacomin, M., Onukwufor, J. O., Schulte, P. M. and Wood, C. M.** (2020). Ionoregulatory aspects of the hypoxia-induced osmoregulatory compromise in the euryhaline Atlantic killifish (*Fundulus heteroclitus*): the effects of salinity. *J. Exp. Biol.* **223**, jeb216309. doi:10.1242/jeb.216309
- Gonzalez, R. J., Wilson, R. W. and Wood, C. M.** (2005). Ionoregulation in tropical fish from ion-poor, acidic blackwaters. In *The Physiology of Tropical Fish, Fish Physiology*, Vol 22 (ed. A. L. Val, V. M. Almeida-Val and D. J. Randall), pp. 397-437. San Diego, CA: Academic Press.
- Gonzalez, R. J., Brauner, C. J., Wang, Y. X., Richards, J. G., Patrick, M. L., Xi, W., Matey, V. and Val, A. L.** (2010). Impact of ontogenetic changes in branchial morphology on gill function in *Arapaima gigas*. *Physiol. Biochem. Zool.* **83**, 322-332. doi:10.1086/648568
- Graham, J. B.** (1997). *Air-Breathing Fishes: Evolution, Diversity, and Adaptation*. London: Academic Press.
- Heisler, N.** (1982). Intracellular and extracellular acid-base regulation in the tropical fresh-water teleost fish *Synbranchus marmoratus* in response to the transition from water breathing to air breathing. *J. Exp. Biol.* **99**, 9-28.
- Hickman, C. P., Jr and Trump, B. F.** (1969). The kidney. In *Fish Physiology*, Vol. 1 (ed. W. S. Hoar and D. J. Randall), pp. 91-239. New York: Academic Press.
- Hills, A. G.** (1973). *Acid-Base Balance: Chemistry, Physiology, Pathophysiology*. Williams & Wilkins.
- Hochachka, P. W., Moon, T. W., Bailey, J. and Hulbert, W. C.** (1978). The osteoglossid kidney: correlations of structure, function, and metabolism with transition to air breathing. *Can. J. Zool.* **56**, 820-832. doi:10.1139/z78-114
- Hulbert, W. C., Moon, T. W., Bailey, J. and Hochachka, P. W.** (1978a). The occurrence and possible significance of chloride-like cells in the nephron of Amazon fishes. *Can. J. Zool.* **56**, 833-844. doi:10.1139/z78-115
- Hulbert, W. C., Moon, T. W. and Hochachka, P. W.** (1978b). The osteoglossid gill: correlations of structure, function, and metabolism with transition to air breathing. *Can. J. Zool.* **56**, 801-808. doi:10.1139/z78-111
- Hunn, J. B.** (1985). Role of calcium in gill function in freshwater fishes. *Comp. Biochem. Physiol.* **82A**, 543-547. doi:10.1016/0300-9629(85)90430-X
- Hunn, J. B. and Willford, W. A.** (1970). The effect of anesthetization and urinary bladder catheterization on renal function of rainbow trout. *Comp. Biochem. Physiol.* **33**, 805-812. doi:10.1016/0010-406X(70)90029-0
- Hyde, D. A. and Perry, S. F.** (1989). Differential approaches to blood acid-base regulation during exposure to prolonged hypercapnia in two freshwater teleosts: the rainbow trout (*Salmo gairdneri*) and the American eel (*Anguilla rostrata*). *Physiol. Zool.* **62**, 1164-1186. doi:10.1086/physzool.62.6.30156207
- Iftikar, F. I., Matey, V. and Wood, C. M.** (2010). The ionoregulatory responses to hypoxia in the freshwater rainbow trout *Oncorhynchus mykiss*. *Physiol. Biochem Zool.* **83**, 343-355. doi:10.1086/648566
- Johansen, K., Mangum, C. P. and Weber, R. E.** (1978). Reduced blood O₂ affinity associated with air breathing in osteoglossid fishes. *Can. J. Zool.* **56**, 891-897. doi:10.1139/z78-124
- Jonz, M. G.** (2018). Insights into the evolution of polymodal chemoreceptors. *Acta Histochem.* **120**, 623-629. doi:10.1016/j.acthis.2018.08.008
- Jonz, M. G. and Zaccone, G.** (2009). Nervous control of the gills. *Acta Histochem.* **111**, 207-216. doi:10.1016/j.acthis.2008.11.003
- King, P. A. and Goldstein, L.** (1983). Renal ammonia excretion and production in goldfish, *Carassius auratus*, at low environmental pH. *Am. J. Physiol.* **245**, R590-R599. doi:10.1152/ajpregu.1983.245.4.R590
- Kinne, R., Kinne-Saffran, E., Schütz, H. and Schölermann, B.** (1986). Ammonium transport in medullary thick ascending limb of rabbit kidney: involvement of the Na⁺, K⁺, Cl⁻-co-transporter. *J. Membr. Biol.* **94**, 279-284. doi:10.1007/BF01869723
- Kültz, D. and Somero, G. N.** (1995). Osmotic and thermal effects on *in situ* ATPase activity in permeabilized gill epithelial cells of the fish *Gillichthys mirabilis*. *J. Exp. Biol.* **198**, 1883-1894.
- Lawrence, M. J., Wright, P. A. and Wood, C. M.** (2015). Physiological and molecular responses of the goldfish kidney (*Carassius auratus*) to metabolic acidosis, and potential mechanisms of renal ammonia transport. *J. Exp. Biol.* **218**, 2124-2135. doi:10.1242/jeb.117689
- Mackay, W. C. and Beatty, D. D.** (1968). The effect of temperature on renal function in the white sucker fish, *Catostomus commersonii*. *Comp. Biochem. Physiol.* **26**, 235-245. doi:10.1016/0010-406X(68)90328-9
- Maetz, J.** (1956). Les échanges de sodium chez le poisson *Carassius auratus* L. Action d'un inhibiteur de l'anhydrase carbonique. *J. Physiol. (Paris)* **48**, 1085-1099.
- Maetz, J.** (1972). Branchial sodium exchange and ammonia excretion in the goldfish *Carassius auratus*. Effects of ammonia-loading and temperature changes. *J. Exp. Biol.* **56**, 601-620.
- Mangum, C. P., Haswell, M. S., Johansen, K. and Towle, D. W.** (1978). Inorganic ions and pH in the body fluids of Amazon animals. *Can. J. Zool.* **56**, 907-916. doi:10.1139/z78-126
- Marshall, W. S.** (2003). Rapid regulation of NaCl secretion by estuarine teleost fish: coping strategies for short duration freshwater exposures. *Biochim. Biophys. Acta* **1618**, 95-105. doi:10.1016/j.bbame.2003.10.015
- Matey, V., Iftikar, F. I., De Boeck, G., Scott, G. R., Sloman, K. A., Almeida-Val, V. M. F., Val, A. L. and Wood, C. M.** (2011). Gill morphology and acute hypoxia: responses of mitochondria-rich, pavement, and mucous cells in two species with very different approaches to the osmo-respiratory compromise, the Amazonian oscar (*Astronotus ocellatus*) and the rainbow trout (*Oncorhynchus mykiss*). *Can. J. Zool.* **89**, 307-324. doi:10.1139/z11-002
- McDonald, D. G. and Rogano, M. S.** (1986). Ion regulation by the rainbow trout, *Salmo gairdneri*, in ion-poor water. *Physiol. Zool.* **59**, 318-331. doi:10.1086/physzool.59.3.30156103
- McDonald, D. G. and Wood, C. M.** (1981). Branchial and renal acid and ion fluxes in the rainbow trout, *Salmo gairdneri*, at low environmental pH. *J. Exp. Biol.* **93**, 101-118.
- Nakada, T., Zandi-Nejad, K., Kurita, Y., Kudo, H., Broumand, V., Kwon, C. Y., Mercader, A., Mount, D. B. and Hirose, S.** (2005). Roles of Slc13a1 and Slc26a1 sulfate transporters of eel kidney in sulfate homeostasis and osmoregulation in freshwater. *Am. J. Physiol.* **289**, R575-R585. doi:10.1152/ajprenal.00725.2004
- Pelster, B. and Wood, C. M.** (2018). Ionoregulatory and oxidative stress issues associated with the evolution of air-breathing. *Acta Histochem.* **120**, 667-679. doi:10.1016/j.acthis.2018.08.012
- Pelster, B., Wood, C. M., Braz-Moto, S. and Val, A. L.** (2020a). Gills and air-breathing organ in O₂ uptake, CO₂ excretion, N-waste excretion, and ionoregulation in small and large pirarucu (*Arapaima gigas*). *J. Comp. Physiol. B.* **190**, 569-583. doi:10.1007/s00360-020-01286-1
- Pelster, B., Wood, C. M., Campos, D. F. and Val, A. L.** (2020b). Cellular oxygen consumption, ROS production and ROS defense in two different size-classes of an Amazonian obligate air-breathing fish (*Arapaima gigas*). *PLoS ONE* **15**, e0236507. doi:10.1371/journal.pone.0236507
- Pitts, R. F.** (1963). *Physiology of the Kidney and Body Fluids*. Year Book Medical Publishers.
- Rahmatullah, M. and Boyde, T. R. C.** (1980). Improvements in the determination of urea using diacetyl monoxime; methods with and without deproteinisation. *Clin. Chim. Acta* **107**, 3-9. doi:10.1016/0009-8981(80)90407-6
- Ramos, C. A., Fernandes, M. N., da Costa, O. T. F. and Duncan, W. P.** (2013). Implications for osmoregulatory compromise by anatomical remodeling in the gills of *Arapaima gigas*. *Anat. Rec.* **296**, 1664-1675. doi:10.1002/ar.22758
- Randall, D. J., Baumgarten, D. and Malysz, M.** (1972). The relationship between gas and ion transfer across the gills of fishes. *Comp. Biochem. Physiol.* **A41**, 629-637. doi:10.1016/0300-9629(72)90017-5

- Randall, D. J., Farrell, A. P. and Haswell, M. S. (1978). Carbon dioxide excretion in the pirarucu (*Arapaima gigas*), an obligate air-breathing fish. *Can. J. Zool.* **56**, 977-982. doi:10.1139/z78-136
- Randall, D. J., Brauner, C. and Wilson, J. (1996). Acid excretion in Amazonian fish. In *Physiology and Biochemistry of the Fishes of the Amazon* (ed. A. L. Val, V. M. F. Almeida-Val and D. J. Randall), pp. 91-100. Manaus, Brazil: INPA.
- Randall, D. J., Wilson, J. M., Peng, K. W., Kok, T. W. K., Kuah, S. S. L., Chew, S. F. and Ip, Y. K. (1999). The mudskipper, *Periophthalmodon schlosseri*, actively transports NH_4^+ against a concentration gradient. *Am. J. Physiol.* **277**, R1562-R1567. doi:10.1152/ajpregu.1999.277.6.R1562
- Rasera, M. F. F. L., Krusche, A. V., Richey, J. E., Ballester, M. V. and Victória, R. L. (2013). Spatial and temporal variability of pCO_2 and CO_2 efflux in seven Amazonian rivers. *Biogeochemistry* **116**, 241-259. doi:10.1007/s10533-013-9854-0
- Robertson, L. M., Val, A. L., Almeida-Val, V. and Wood, C. M. (2015). Ionoregulatory aspects of the osmorepiratory compromise during acute environmental hypoxia in 12 tropical and temperate teleosts. *Physiol. Biochem. Zool.* **88**, 357-370. doi:10.1086/681265
- Soares, J. M., Beletti, M. E. and Santos, A. L. Q. (2006). Ultrastructural study of the pirarucu swim-bladder (*Arapaima gigas*). *Vet. Not. Uberlândia* **12**, 55-61.
- Scadenga, M., McKenzie, C., He, W., Bartsch, H., Dubowitz, D. J., Stec, D. and Leger, J. S. (2020). Morphology of the Amazonian teleost genus *Arapaima* using advanced 3D imaging. *Front. Physiol.* **11**, 260. doi:10.3389/fphys.2020.00260
- Scott, G. R., Wood, C. M., Sloman, K. A., Iftikar, F. I., De Boeck, G., Almeida-Val, V. M. F. and Val, A. L. (2008). Respiratory responses to progressive hypoxia in the Amazonian oscar, *Astronotus ocellatus*. *Respir. Physiol. Neurobiol.* **162**, 109-116. doi:10.1016/j.resp.2008.05.001
- Smith, H. W. (1959). *From Fish to Philosopher. The Story of Our Internal Environment*. Revised edition. Chicago: Ciba.
- Stevens, E. D. and Holeyton, G. F. (1978). The partitioning of oxygen uptake from air and from water by the large obligate air-breathing teleost pirarucu (*Arapaima gigas*). *Can. J. Zool.* **56**, 974-976. doi:10.1139/z78-135
- Sundin, L. and Nilsson, S. (2002). Branchial innervation. *J. Exp. Zool.* **293**, 232-248. doi:10.1002/jez.10130
- Tavares-Dias, M., Barcellos, J. F. Marcon, J. L. Menezes, G. C., Ono, E. A. and Affonso, E. G. (2007). Hematological and biochemical parameters for the pirarucu *Arapaima gigas* Schinz, 1822 (Osteoglossiformes, Arapaimatidae) in net cage culture. *Electronic J. Ichthyol.* **2**, 61-68.
- Thinh, P. V., Huong, D. T. H., Gam, L. T. H., Damsgaard, C., Phuong, N. T., Bayley, M. and Wang, T. (2019). Renal acid excretion contributes to acid-base regulation during hypercapnia in air-exposed swamp eel (*Monopterus albus*). *J. Exp. Biol.* **222**, jeb198259. doi:10.1242/jeb.198259
- Val, A. L. and Almeida-Val, V. M. F. (1995). *Fishes of the Amazon and their Environment*. Heidelberg, New York: Springer-Verlag, Berlin.
- Verdouw, H., van Eched, C. J. A. and Dekkers, E. M. J. (1978). Ammonia determination based on indophenol formation with sodium salicylate. *Water Res.* **12**, 399-402. doi:10.1016/0043-1354(78)90107-0
- Wolf, K. (1963). Physiological salines for fresh-water teleosts. *Progressive Fish Cult.* **25**, 135-140. doi:10.1577/1548-8659(1963)25[135:PSFFT]2.0.CO;2
- Wood, C. M. (1992). Flux measurements as indices of H^+ and metal effects on freshwater fish. *Aquat. Toxicol.* **22**, 239-264. doi:10.1016/0166-445X(92)90043-M
- Wood, C. M. (1993). Ammonia and urea metabolism and excretion. In *The Physiology of Fishes* (ed. D. Evans), pp. 379-425. Boca Raton: CRC Press.
- Wood, C. M. (1995). Excretion. In *Physiological Ecology of the Pacific Salmon* (ed. C. Groot, L. Margolis and W. C. Clarke), pp. 381-438. Vancouver: Government of Canada Special Publications Branch, UBC Press.
- Wood, C. M. and Patrick, M. L. (1994). Methods for assessing kidney and urinary bladder function in fish. In *Biochemistry and Molecular Biology of Fishes*, Vol. 3 (ed. P. W. Hochachka and T. P. Mommsen), pp. 127-143. New York: Elsevier.
- Wood, C. M., Milligan, C. L. and Walsh, P. J. (1999). Renal responses of trout to chronic respiratory and metabolic acidoses and metabolic alkalosis. *Am. J. Physiol.* **277**, R482-R492. doi:10.1152/ajpregu.1999.277.2.R482
- Wood, C. M., Kajimura, K., Sloman, K. A., Scott, G. R., Almeida-Val, V. M. F. and Val, A. L. (2007). Rapid regulation of Na^+ and ammonia fluxes in response to acute environmental hypoxia in the Amazonian oscar, *Astronotus ocellatus*. *Am. J. Physiol.* **292**, R2048-R2058. doi:10.1152/ajpregu.00640.2006
- Wood, C. M., Iftikar, F. I., Scott, G. R., De Boeck, G., Sloman, K. A., Matey, V., Valdez Domingos, F. A., Mendonça Duarte, R., Almeida-Val, V. M. F. and Val, A. L. (2009). Regulation of gill transcellular permeability and renal function during acute hypoxia in the Amazonian oscar (*Astronotus ocellatus*): new angles to the osmo-respiratory compromise. *J. Exp. Biol.* **212**, 1949-1964. doi:10.1242/jeb.028464
- Wood, C. M., Pelster, B., Giacomin, M., Sadauskas-Henrique, H., Almeida-Val, V. M. and Val, A. L. (2016). The transition from water-breathing to air-breathing is associated with a shift in ion uptake from gills to gut: a study of two closely related erythrinid teleosts, *Hoplerethrinus unitaeniatus* and *Hoplias malabaricus*. *J. Comp. Physiol.* **B186**, 431-445. doi:10.1007/s00360-016-0965-5
- Wood, C. M., de Souza Netto, J. G., Wilson, J. M., Duarte, R. M. and Val, A. L. (2017). Nitrogen metabolism in tambaqui (*Colossoma macropomum*), a neotropical model teleost: hypoxia, temperature, exercise, feeding, fasting, and high environmental ammonia. *J. Comp. Physiol. B.* **186**, 431-445. doi:10.1007/s00360-016-0965-5
- Wood, C. M., Ruhr, I. M., Schauer, K. L., Wang, Y., Mager, E. M., McDonald, D., Stanton, B. and Grosell, M. (2019). The osmorepiratory compromise in the euryhaline killifish: water regulation during hypoxia. *J. Exp. Biol.* **222**, jeb204818. doi: 10.1242/jeb.204818
- Wright, P. A., Wood, C. M. and Wilson, J. M. (2014). Rh versus pH: the role of Rhesus glycoproteins in renal ammonia excretion during metabolic acidosis in a freshwater teleost fish. *J. Exp. Biol.* **217**, 2855-2865. doi:10.1242/jeb.098640
- Yellen, G. (1987). Permeation in potassium channels: implications for channel structure. *Ann. Rev. Biophys. Chem.* **16**, 227-246. doi:10.1146/annurev.bb.16.060187.001303
- Zaccane, G., Cupello, C., Capillo, G., Kuciel, M., Nascimento, A. L., Gopesh, A., Germanà, G. P., Spanò, N., Guerrero, M. C., Aragona, M. et al. (2020). Expression of acetylcholine- and G protein coupled muscarinic receptor in the neuroepithelial cells (NECs) of the obligated air-breathing fish, *Arapaima gigas* (Arapaimatidae: Teleostei). *Zoology* **139**, 125755. doi:10.1016/j.zool.2020.125755
- Zall, D. M., Fisher, D. and Garner, M. Q. (1956). Photometric determination of chloride in water. *Anal. Chem.* **28**, 1665-1668. doi:10.1021/ac60119a009